UAB

FRACTUS ANTENNAS

Master's Thesis

Master in Telecommunication Engineering

4G Antenna Solution for Small Wireless Platforms

Namir Saffour Jendi

Master's Thesis Directors: Dr. Aurora Andújar and *Dr. Jaume Anguera*
From Fractus Antennas

Supervisor UAB: Josep Parron Granados

Department of Telecommunication and Systems Engineering

Escola d'Enginyeria
Universitat Autònoma de Barcelona (UAB)

July 2019

UAB

El tribunal d'avaluació d'aquest Treball Fi de Màster, reunit el dia _____, ha acordat concedir la següent qualificació:

President: _____

Vocal: _____

Secretari: _____

Els sotasignants, **Josep Parron Granados**, Professor de l'Escola d'Enginyeria de la Universitat Autònoma de Barcelona (UAB), i **Aurora Andújar Linares** i **Jaume Anguera Pros**, tutors de l'alumne a l'empresa **Fractus Antennas** i directors del projecte.

CERTIFIQUEN:

Que el projecte presentat en aquesta memòria de Treball Fi de Màster ha estat realitzat sota la seva supervisió per l'alumne **Namir Saffour Jendi**.

I, perquè consti a tots els efectes, signen el present certificat.

Bellaterra, 2 de Juliol de 2019.

Signatures:

Aurora Andújar Linares Jaume Anguera Pros Josep Parron Granados

Resum:

En aquest projecte s'explora la solució activa per millorar el rendiment de plataformes sense fils petites.

Amb aquest propòsit, s'ha fet un benchmarking *per determinar què considerar com a plataforma sense fils petita. Després d'això, s'ha estudiat l'efecte de la longitud del pla de massa sobre el rendiment del sistema per, finalment, implementar la solució activa per veure la millora que ofereix respecte a una xarxa d'adaptació multibanda.*

Resumen:

En este proyecto se explora la solución activa para mejorar el rendimiento de plataformas inalámbricas pequeñas.

Para ello, se ha hecho un benchmarking *para determinar qué considerar como plataforma pequeña. Después de esto, se ha estudiado el efecto de la longitud del plano de masa sobre el rendimiento del sistema para, finalmente, implementar la solución activa para ver la mejora que ofrece respecto a una red de adaptación multibanda.*

Summary:

In this project it is explored the active solution to improve the performance of small wireless platforms.

To do so, a benchmarking is made to determine what dimensions to consider as small platform. After that, it is studied the impact of the ground plane length on the performance of the system to, finally, implement the active solution to see the improvement that it offers respect to a multiband matching network.

To my family. And the family.
To the gone.

ACKNOWLEDGEMENT

Thanks to all and each of the people who has contributed directly or indirectly, intentionally or unintentionally. Thanks to the ones who encouraged me and who motivated me. Thanks to who was present along this challenge and the coming.

Special thanks to my two Master Thesis directors, Dr. Aurora Andújar and Dr. Jaume Anguera, for their help, support and patience guiding me along this project.
Thanks also to Josep Parron for his support and disposition to help as my academic supervisor and teacher.

Thanks to Fractus Antennas S.A. for giving me the opportunity to develop this project with them in their installations. Thank you for your trust in me and confidence.

This has only just begun.

El truco está en la rosca.

TABLE OF CONTENTS

LIST OF TABLES

LIST OF FIGURES

1. INTRODUCTION

Since some decades ago, there is a growing interest in the wireless communications coming from the continuous increase of connected devices and, consequently, the need of reducing the number of existing wires.

This reduction of the number of wires, apart from being aesthetically more pleasant, allows everything to be connected to make everything easier and more comfortable for people to control devices remotely. For instance, be able to check your mobile phone notifications through your smartwatch or to turn on the air conditioner without looking for its remote controller is faster than taking your phone out of your pocket or than finding the remote controller. To be wireless, these "smart" devices must integrate antennas, which substitute the functionality of communications of the wires.

Continuing with the comfort topic, it wouldn't be comfortable at all to have, for instance, a large and heavy smartwatch tied on the wrist, so the size trend of those devices is to make them small. This means that the batteries that feed those devices will be small too, so low consumption is a main target when designing them.

Two approaches can be made from the previous statement: the first one is that low range for communications is assumed and accepted. The alternative approach is that the working frequencies should be at the lower frequency bands, which is more desirable when, for instance, you send a message to a friend, which has to reach a base station to travel to be routed to the receiver.

The problem of working on low frequencies is that it is hard to achieve a good performance in small platforms. This means the transmission power should be higher in order to obtain good communication ranges, but by doing this the duration of the device battery would be decreased, which goes against the low consumption target.

What is developed along this thesis is an alternative to improve the performance of the system in terms of efficiency without increasing the transmission power, which consists in using an active solution simulating the effect of the switches and selective narrow-band matching networks.

1.1. Some relevant parameters

- Reflection coefficient: Ratio of reflected voltage wave respect to the input voltage wave. Along this project, it will be used the reflection coefficient and the return loss (or S_{11}) indistinctly.

$$Reflection\ coefficient = \frac{Reflected\ voltage\ wave}{Input\ voltage\ wave}$$

$$S_{11}\ (dB) = 20\log\left(\frac{Reflected\ voltage\ wave}{Input\ voltage\ wave}\right)$$

Example:
If $S_{11}\ (dB) = -6\ dB$,
then 25% of the wave is reflected, 75% of the wave is delivered to the antenna.

- Radiation efficiency (η_r): Ratio of the radiated power respect to the accepted power by the antenna considering the losses that the matching network components introduce.

- Antenna/Total efficiency (η_a): Ratio of the radiated power respect to the available power by the antenna considering the mismatch losses and other losses that the system introduces.

$$\eta_a = \eta_r\ (1 - |S_{11}|^2)$$

The objective is to maximize the antenna efficiency (η_a). This is achieved maximizing the matching (ideally $S_{11} = 0$) and choosing the best components in terms of the Q-factor (maximizing the radiation efficiency, η_r).

1.2. Objectives

The main objective of this project is to design a 4G antenna solution with efficiencies over 30% for wireless platforms having a small PCB size.
It is understood as small PCB as the one which have representative dimensions for Fleet Management, Modules, OBDs (On Board Diagnostics) or IoT devices' applications.
To determine these dimensions, as well as the 4G frequency bands that will be considered, a study will be done taking into account devices that can currently be found in the market.

1.3. Project structure

The project is divided in three main parts:

The first of them consists in a study/benchmarking of the Fleet Management, Modules, OBDs and IoT devices. This will allow to delimit the aspects to consider along this project, as well as establishing some reference values for the development of the following two main parts, as the frequency bands and the dimensions of the devices. A part of the analyzed devices can be currently found in the market, while the rest of them are still in the design stage.

The second part is a study regarding the impact of the length of the ground plane of a PCB on the performance, in terms of efficiency, of the device. In this way, the obtained results can be extrapolated to intuit what to expect on the next part of the project. The bands to cover on this part will be determined by what is extracted from the first part.

The last main part of this project consists in exploring a technique to improve the efficiency for a determined PCB size. It will be developed for the Fleet Management PCB size, which will be extracted from the study carried out in the benchmarking part.

1.4. Methodology

The followed methodology to carry out this project (Figure 4) has consisted, in first place, in detecting a trend of the market to make the PCBs of wireless devices smaller. This point creates a rising interest in researching and applying techniques to improve their performance.

Once this necessity has been identified, it is needed a search for information related with the topic of the project, such as documents that help to understand the principle of functioning of the technology to use, previous work and state of the art to know what is currently being done regarding the scope of the project, and techniques that could be used to improve the performance of the system.

Also, electromagnetic simulations had to be done along the project. These electromagnetic simulations have been carried out to explore diverse scenarios without the complexity of having to implement them.
The used electromagnetic simulator is CST [1], owned by Dassault Systemes, which is available in Fractus Antennas' laboratory. This simulator has different solvers available, including the time domain solver, which has been used for the development of this project.

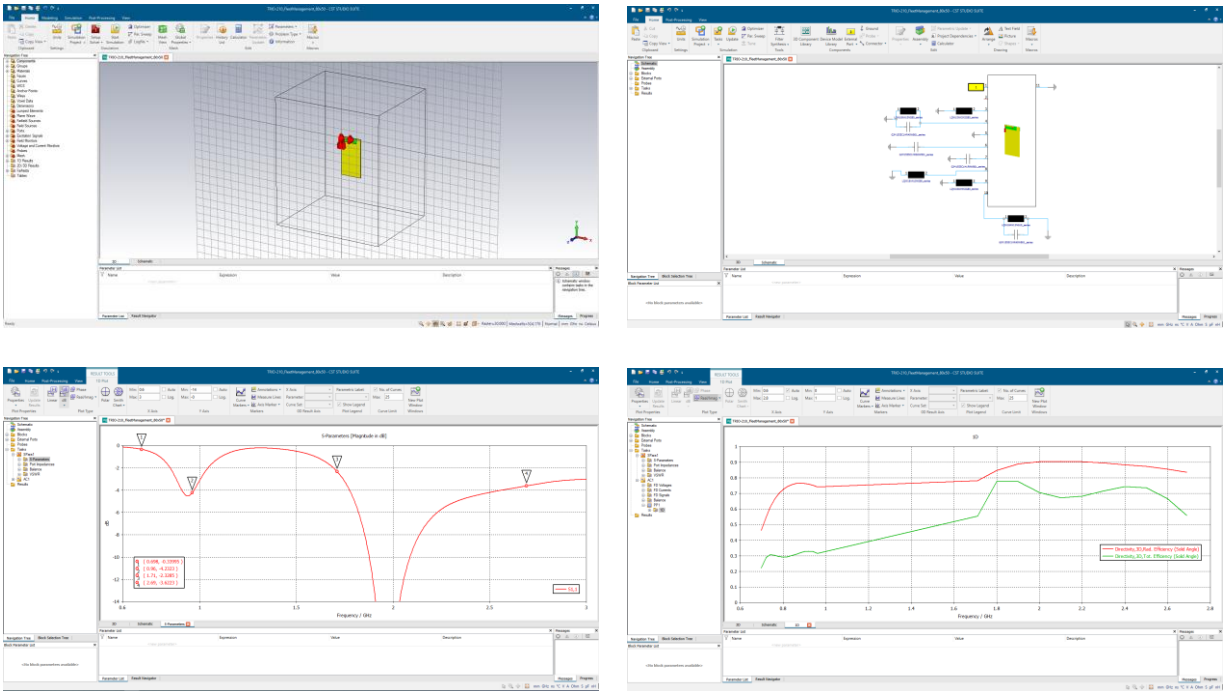

Figure 1 – CST screenshots.

Another kind of tasks that have been carried out is the prototyping and measurements.
For preparing the prototypes, it has been used the mechanical laboratory of Fractus Antennas (from now on, NN).
For designing of the matching networks and the measurements, it has been used two different JBC soldering tools: the first one is the regular size station, used for roughly solder; the second one is a micro station, for more precise tasks as placing components.
To check the reflection coefficient of the prototypes, it has been used a RHODE & SCHWARZ ZVRE, which is a two port VNA, available to measure starting from 9 KHz up to 4 GHz.

Figure 2 – RHODE & SCHWARZ's ZVRE VNA.

The efficiency of the prototypes has been measured using the SATIMO Stargate 32 anechoic chamber, which has 31 probes and a rotating platform to acquire full 3D field data. It can measure from 700 MHz up to 6 GHz.

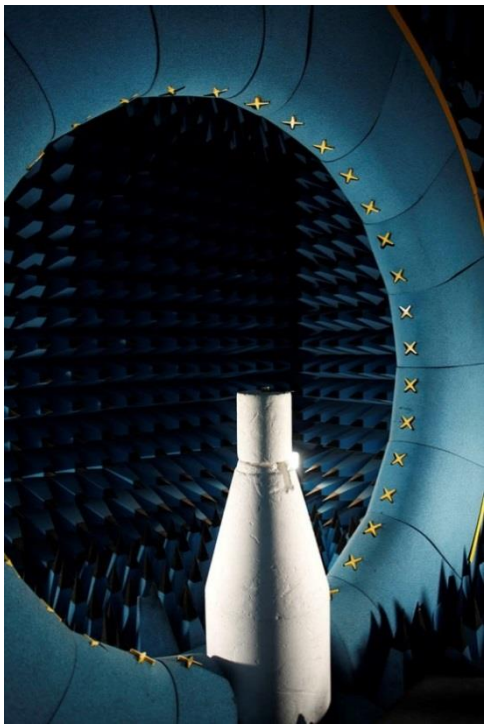

Figure 3 – SATIMO Stargate 32

All the mentioned tools and utilities in this section that have been used are available in NN's laboratory.

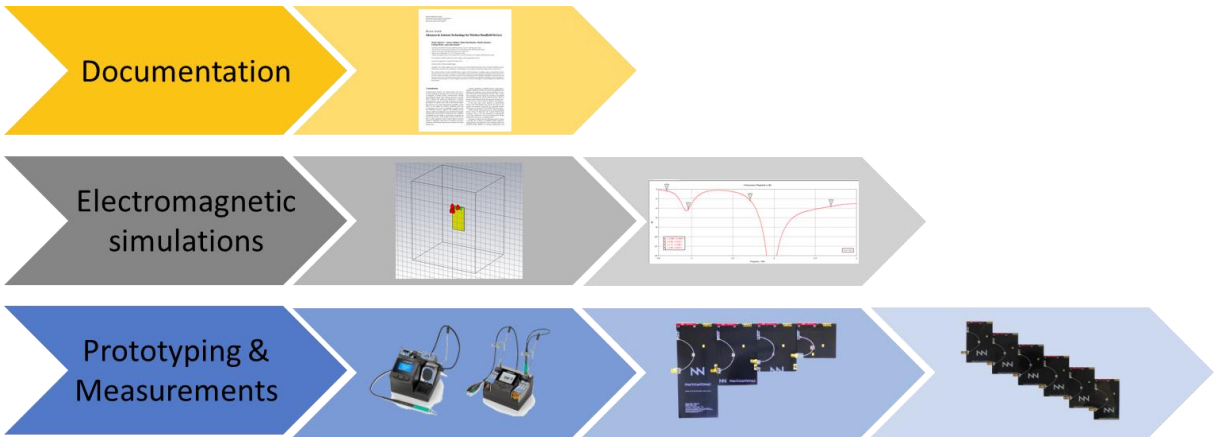

Figure 4 – Description of the working methodology followed to carry out this project.

2. BENCHMARKING

2.1. Introduction

In this chapter it is going to be presented the benchmarking that has been carried out in order to analyze some of the typical specifications of the Fleet Management, Modules, OBDs and IoT devices.
The two significant specifications that are taken into account in the analysis are the dimensions of the device and the frequency bands that covers.

2.2. Fleet Management, Modules, OBDs and IoT devices

51 devices for the applications of interest are analyzed to extract the needed parameters. In Table 1 is shown the list of the devices separated per application. From each of the devices, it has been extracted its PCB dimensions and the frequency bands that covers.

Application	Device name	Manufacturer	Bands of operation	Length (mm)	Width (mm)
Fleet management	GPS2000C	ViTech	2G GSM / 3G WCDMA	70	47
	BT 500	ORBCOMM	BT / GNSS / WiFi / 2G / 3G / LTE	140	105
	Piccolo STX	Wireless Links	BT / GPS / 2G / 3G / 4G	85	52
Modules	XB3-C-A2-UT-001	Digi International	LTE(699-960MHz; 1710-2170MHz) / BT	25	33
	RN2483A-I/RM104	Microchip Technology	LoraWAN (433MHz; 863-870MHz)	17,8	26,7
	XBC-M5-UT-001	Digi International	3G (800MHz, 850MHz, 900MHz, 1900MHz, 2100MHz)	25	33
	XB8X-DMUS-001	Digi International	ISM-868MHz	33,8	22,1
	NRF52832	Nordic Semiconductor	BT	20	20
	Device #1			65	42
	Device #2			36	14
	Device #3			50	25
	Device #4			24	18
	Device #5			17,5	19
	Device #6			22,5	22
	Device #7			50	50
	Device #8			50	50
	Device #9			83	72
	Device #10			100	40
	Device #11			60	23
	Device #12			48	19
	Device #13			47	34
	Device #14			87	68
OBD	Mini ELM327	Moonar	BT (2.4-2.5GHz)	48	35
	V06H4K-1	KiMood	BT-WiFi (2.4-2.5GHz) / 3G / 4G	43	25
	K880	Kkmoon	BT (2.4-2.5GHz)	47	31
	NOBD2BT	iLC	BT-WiFi (2.4-2.5GHz) / 3G / 4G		
	GPS2000C	ViTech	2G GSM / 3G WCDMA	70	47
	BlueLink ELD	Wireless Links	BT	69	38
	Device #15			55	25
	Device #16			40	40
	Device #17			76	46
	Device #18			48	32
	Device #19			48	38
	Device #20			32	25
	Device #21			102	72
	Device #22			44	40
IoT devices	AmazFit Bip	Xiaomi	BT / GNSS / WiFi	20	20
	PHOTONH	Particle	WiFI	43	28
	GDK101	FTLAB		59	39
	DM182022	Microchip Technology	BT		
	UG309	Silicon Labs	ZigBee / BT	45	30
	ATAVRBLE-IOT	Microchip Technology	BT		
	1270553	ILT	BT	59	55
	Device #23			62	45
	Device #24			59	52
	Device #25			45	40
	Device #26			149	125
	Device #27			80	80
	Device #28			32,5	32,5
	Device #29			50	30
	Device #30			62	77,5
	Device #31			25	25

Table 1 – List of analyzed devices.

It is seen that most of the devices cover mobile frequency bands. In addition to the mobile bands, they typically are also capable of work on another frequency bands, such as Bluetooth/WiFi, GNSS or ISM bands (Zigbee, LoRa…).

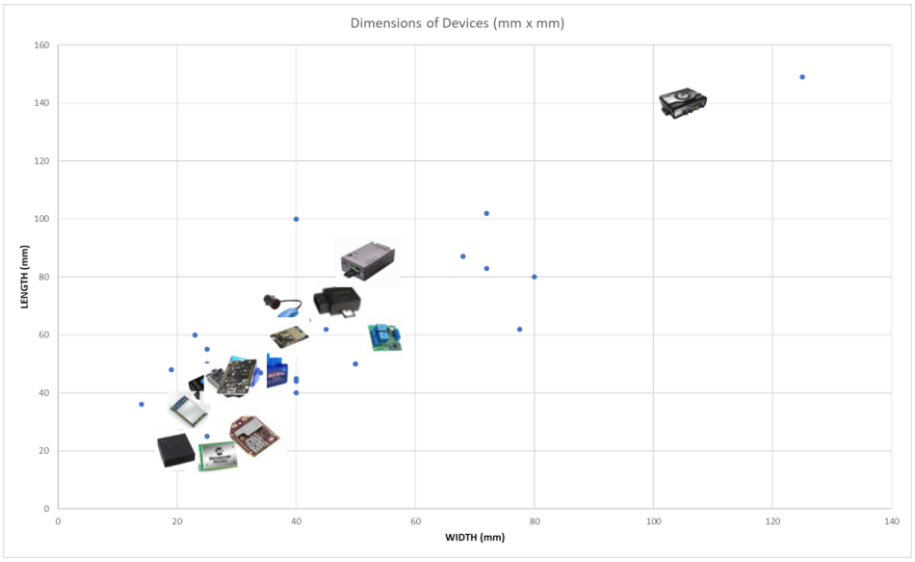

Figure 5 – Analyzed devices for Fleet Management, Modules, OBDs and IoT classified by size.

The size differences between the shown devices in Figure 5 is considerable and no clear trend can be extracted. That's why a classification by application is done in the following subsections.

2.2.1. Fleet Management

In Figure 6, the found Fleet Management devices are presented, which show a clear trend around 80mm x 50mm. One of the devices is far from these dimensions, which makes it less representative in terms of size.

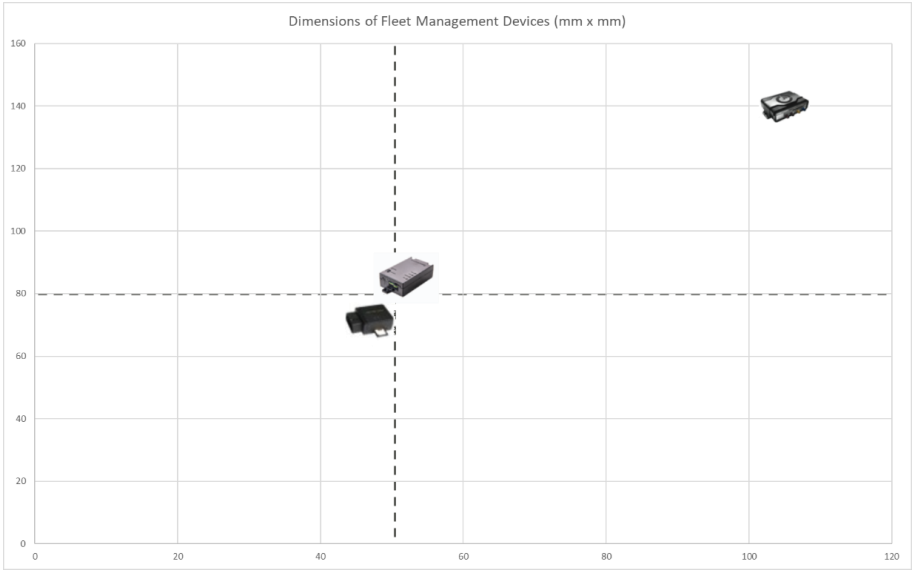

Figure 6 – Analyzed devices for Fleet Management classified by size.

2.2.2. Modules

For the case of the modules (Figure 7), what has been observed is that the trending size of those is around 45mm x 35mm. Three devices are far from these dimensions, which makes them less representative in terms of size.

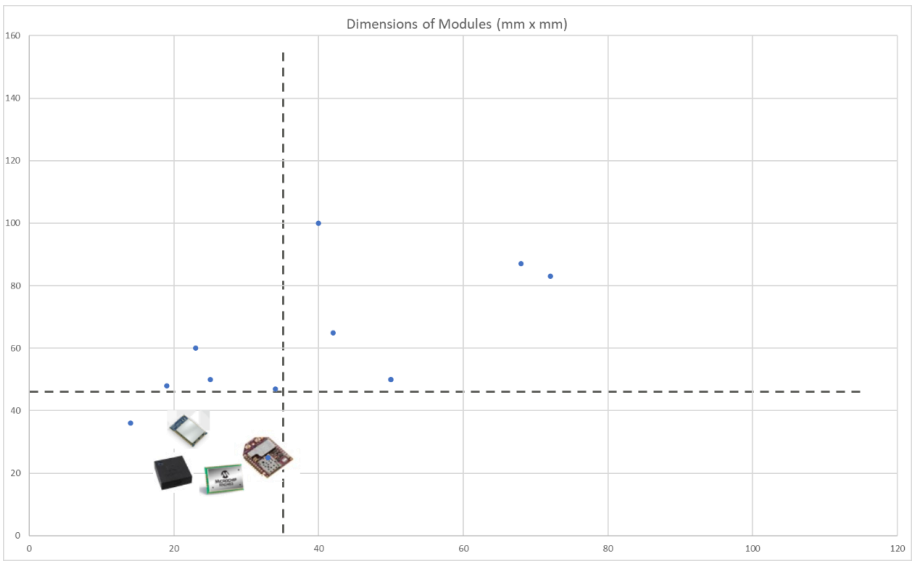

Figure 7 – Analyzed Modules classified by size.

2.2.3. OBDs

When talking about the OBDs, the trend of the devices is making them with a size around 55mm x 40mm (Figure 8). The dimensions of one of the devices are far from this trend, which makes it less representative in terms of size.

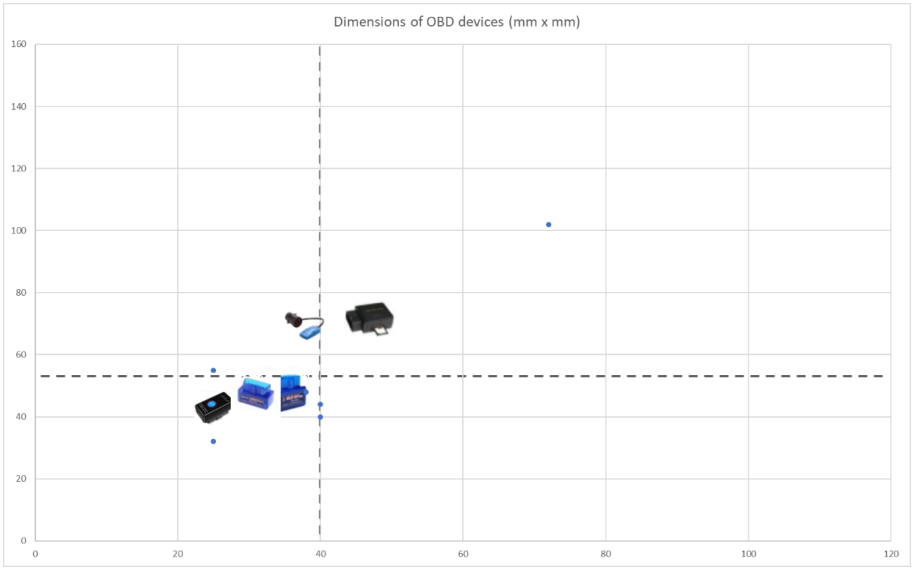

Figure 8 – Analyzed OBDs classified by size.

2.2.4. IoT devices

Finally, for the IoT devices is observed that 55mm x 50mm can be a representative size. Four devices are deviated from these dimensions, which makes them less representative in terms of size.

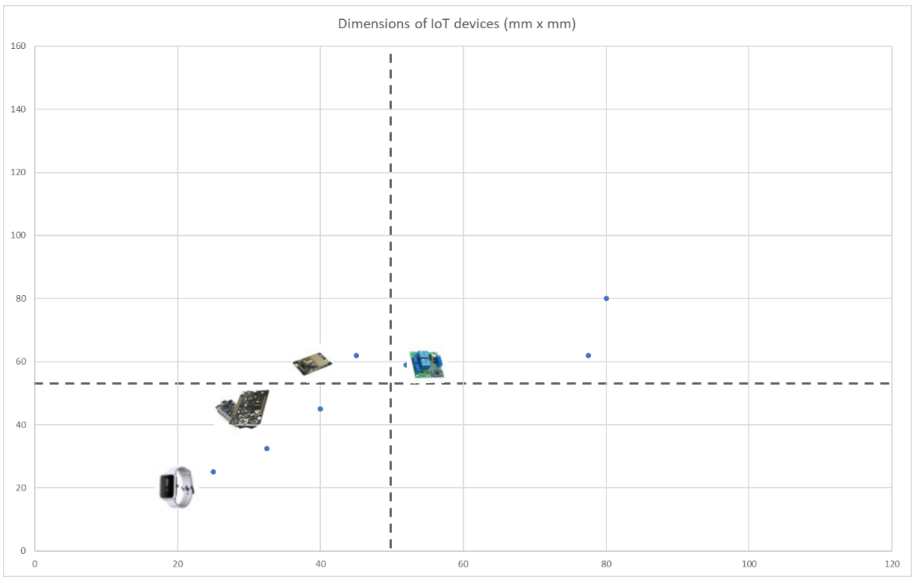

Figure 9 – Analyzed IoT devices classified by size.

2.2.5. Summary

The reference dimensions extracted from the list of devices and the graphs shown along this section for each of the applications of interest are shown in Table 2., which will be considered when needed along this project.

Application	'Reference' size (mm x mm)
Fleet management	80 x 50
Modules	45 x 35
OBDs	55 x 40
IoT devices	55 x 50

Table 2 – Reference size for each of the analyzed application.

The frequency bands covered by most of the analyzed devices consist in some mobile bands (such as 2G, 3G or 4G/LTE services) and a short-range communication service (Bluetooth, WiFi…).

2.3. TRIO mXTEND™ chip antenna component

Since the typical dimensions of the devices for the applications taken into account along this project are restrained, two of the NN products could be considered: the RUN mXTEND™ [2] or the TRIO mXTEND™ [3] [4] [5].
Moreover, it also has to be considered that the frequency ranges to take into account include the 700MHz band, which could be covered by the ALL mXTEND™ [6] or the already introduced TRIO mXTEND™.

Therefore, the TRIO mXTEND™ is the NN product that better suits the kind of devices that are considered along this project since it can cover the lowest of the considered frequencies more efficiently than the RUN mXTEND™ and, at the same time, its dimensions are more restrained than the ALL mXTEND™ ones. These products belong to a new family of products of NN, called Virtual Antenna™ [7]-[34].

2.3.1. Physical specs

The dimensions of the TRIO mXTEND™ are 30mm x 1mm x 1mm. Its structure consists in two access ports, one at each of its short edges, which allow to improve the overall performance or, if applicable, covering another application besides the mobile bands.

Measure	mm
A	142-52
B	130-40
C	60
D	9
E	40
F	20

Tolerance: ±0.2 mm

Material: The Evaluation Boards are built on FR4 substrate. Thickness is 1 mm.

Figure 10 – Evaluation Board for providing operation in 2 frequency ranges, 698 – 960 MHz and 1710 – 2690 MHz.

Clearance Area: 40mm x 12mm (yellow dotted rectangle)

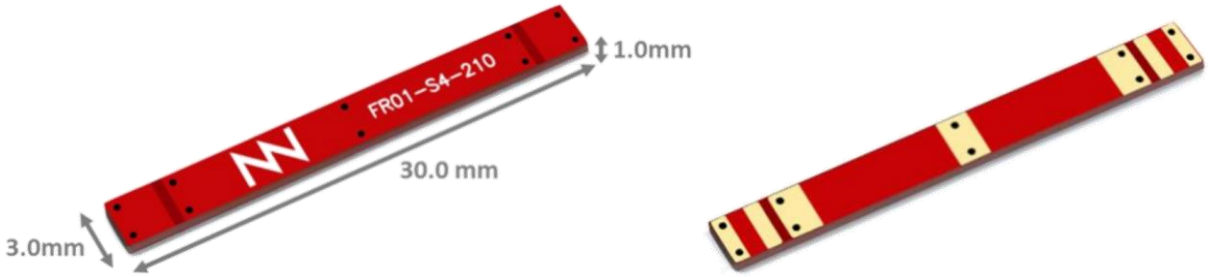

Figure 11 – TRIO mXTEND™ top and bottom view.

In addition, the chip antenna allows to incorporate filters (Figure 12): one for two ports configuration; two for one port configuration. This will allow to optimize the performance on the LFR (Low Frequency Region; 698 – 960 MHz) and HFR (High Frequency Region; 1710 – 2690 MHz), giving the desired importance to each of the bands.

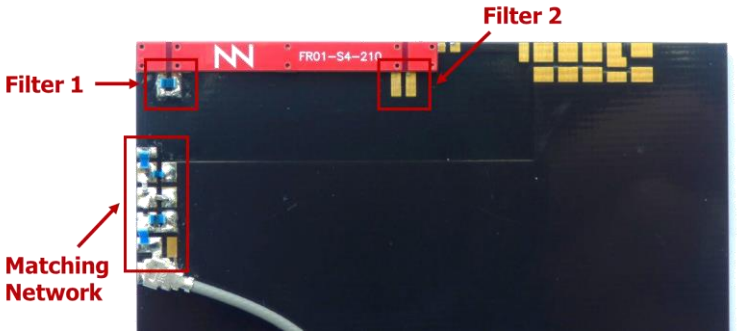

Figure 12 – Filters and Matching network distribution.

2.3.2. Performance analysis

2.3.2.1. Matching network

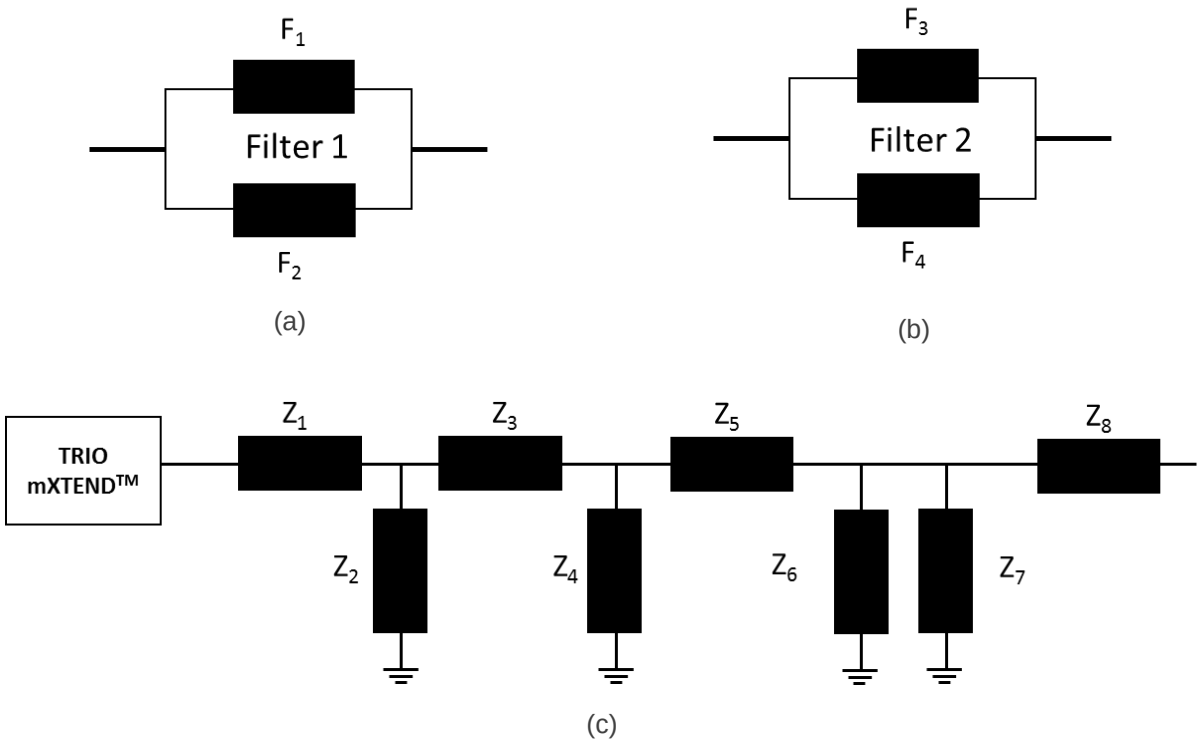

Figure 13 – Topologies for the filters (a,b) and the matching network (c) that are used along the project.

The filters (Figure 13.a Figure 13.b) that are implemented in the TRIO mXTEND™ Evaluation Board are two components filters in notch configuration to have a stopband filter.
The considered topology for the matching network (Figure 13.c), which has been proved to be the optimal to cover the bands of interest.

The values of the filters and the matching network components are shown in Table 3. It is worth to comment that the inductors and capacitors have been selected to get the best quality factor. The quality factor of each of the components can be found in its datasheet [35]. For this project, 0402 and 0603 SMD components from Murata have been chosen.

Component	Value	Part number
F1	15 nH	LQW18AN15NG80
F2	0.3 pF	GJM1555C1HR30WB01
F3	Empty	-
F4	Empty	-
Z1	2.2 nH	LQW18AN2N2C80
Z2	8.6 nH	LQW15AN8N6G80
Z3	2.2 pF	GJM1555C1H2R2WB01
Z4	1 pF	GJM1555C1H1R0WB01
Z5	0Ω	-
Z6	10 nH	LQW18AN10NG80
Z7	0.36 pF	GJM1555C1HR36WB01
Z8	3 nH	LQW18AN3N0C80

Table 3 – Matching network values for the TRIO mXTEND™ in its evaluation board.

2.3.2.2. Reflection coefficient & Efficiency

As a fixed target and a widely accepted value in the RF & Antennas ambit, the TRIO mXTEND™ Evaluation Board presents a VSWR < 3:1 on the frequency ranges of interest (698 – 960 MHz and 1710 – 2690 MHz). This means that the reflection coefficient of a well implemented evaluation board is S_{11} < -6dB for the such said frequency ranges (Figure 14).

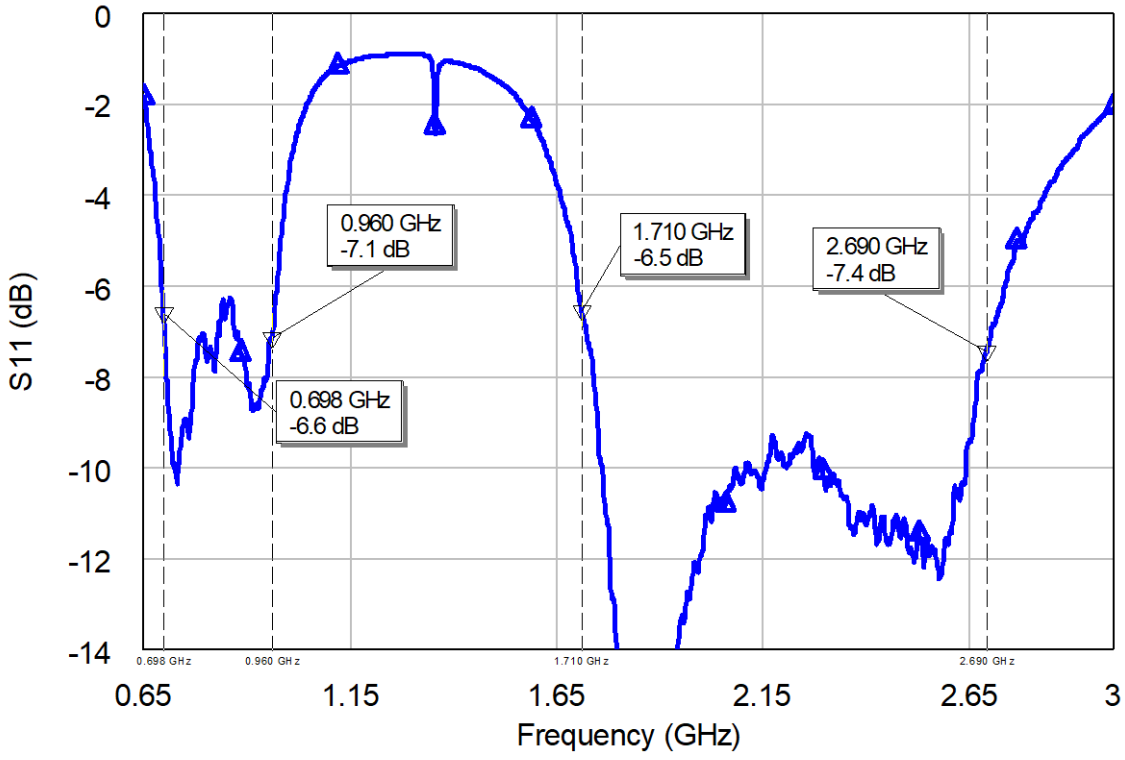

Figure 14 – Typical reflection coefficient for the TRIO mXTEND™ in its evaluation board.

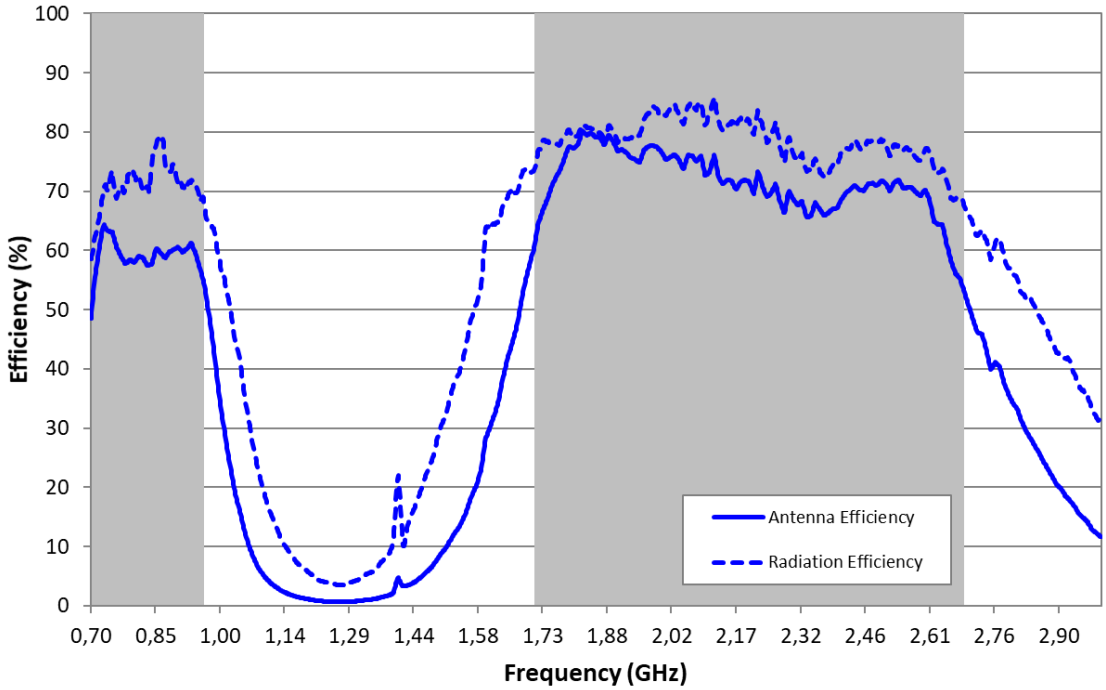

Figure 15 – Typical Antenna and Radiation Efficiency (%) for the TRIO mXTEND™ in its evaluation board.

When talking about the efficiency, it has been determined, for the TRIO mXTEND™ integrated in the PCB in Figure 10 with the matching network in presented in its User Manual [3] (Figure 13, Table 3), that the target antenna efficiency values are >55% for the LFR (698 – 960 MHz) and 65% for the HFR (1710 – 2690 MHz).

2.3.2.3. Radiation patterns

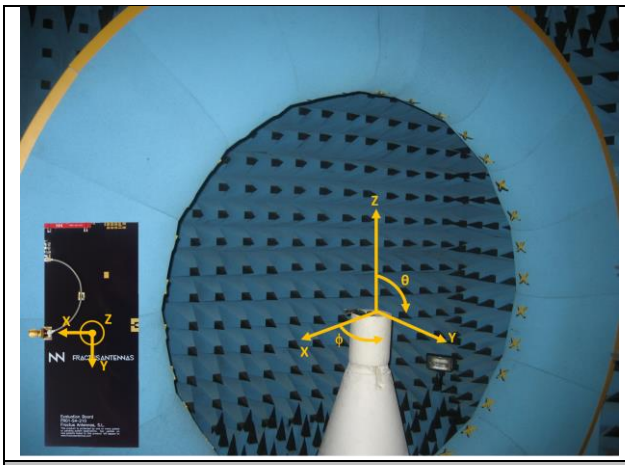

Measurement System Set-Up
Evaluation Board in Plane XY

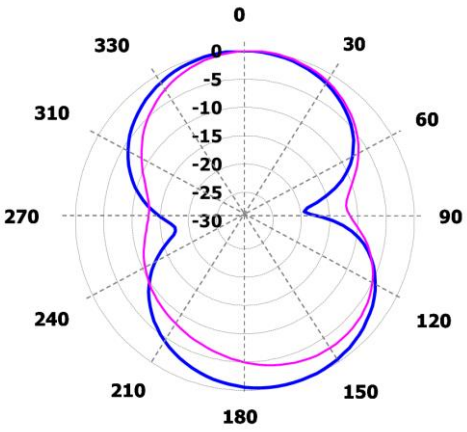

θ = 90º Plane XY at 750 MHz and 890 MHz

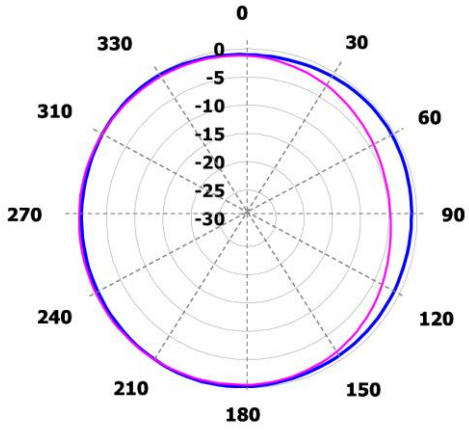

ϕ = 0º Plane XZ at 750 MHz and 890 MHz

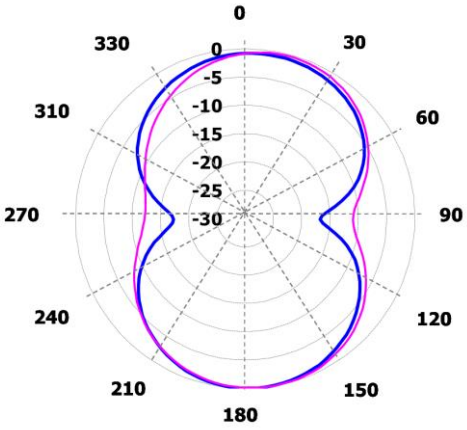

ϕ = 90º Plane YZ at 750 MHz and 890 MHz

Gain	**Peak Gain**	1.1 dBi
	Average Gain across the band	0.5 dBi
	Gain Range across the band (min, max)	-0.7 <–> 1.1 dBi
Efficiency	**Peak Efficiency**	64.3 %
	Average Efficiency across the band	59.3 %
	Efficiency Range across the band (min, max)	48.5 – 64.3 %

Table 4 – Antenna Gain and Total Efficiency from the Evaluation Board (Figure 10) within the 698 – 960 MHz frequency range. Measures made in the Satimo STARGATE 32 anechoic chamber.

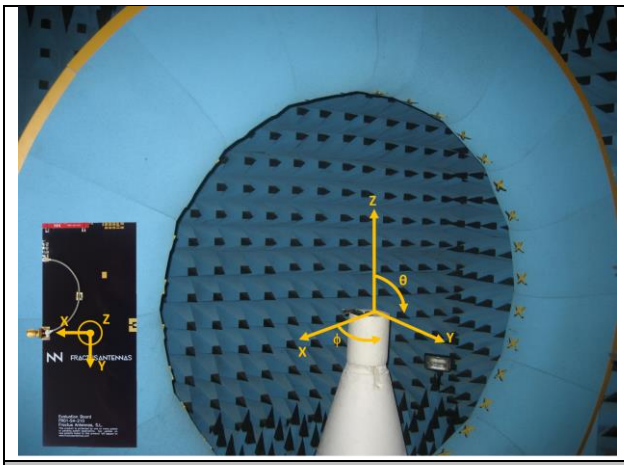

Measurement System Set-Up Evaluation Board in Plane XY

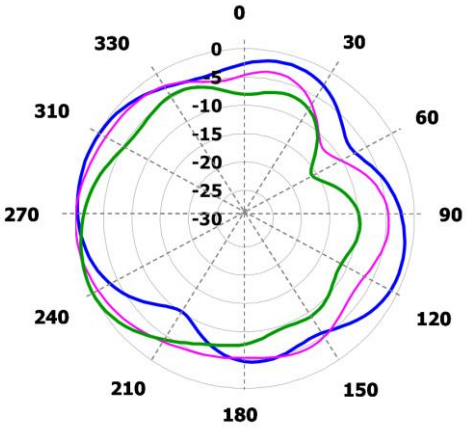

θ = 90º Plane XY at 1.71 GHz, 2.2 GHz and 2.69 GHz

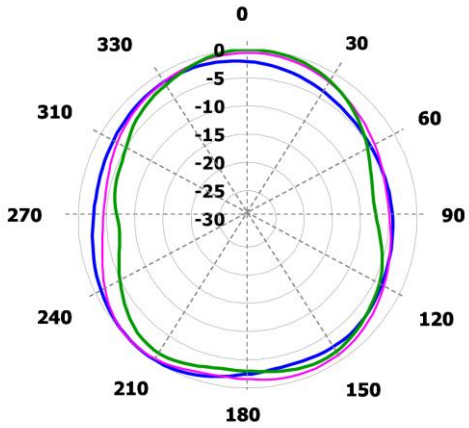

ϕ = 0º Plane XZ at 1.71 GHz, 2.2 GHz and 2.69 GHz

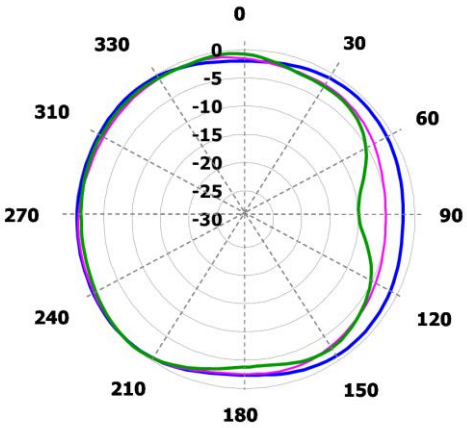

ϕ = 90º Plane YZ at 1.71 GHz, 2.2 GHz and 2.69 GHz

Gain	**Peak Gain**	2.4 dBi
	Average Gain across the band	1.8 dBi
	Gain Range across the band (min, max)	0.3 <–> 2.4 dBi
Efficiency	**Peak Efficiency**	80.2 %
	Average Efficiency across the band	71.4 %
	Efficiency Range across the band (min, max)	52.9 – 80.2 %

Table 5 – Antenna Gain and Total Efficiency from the Evaluation Board (Figure 10) within the 1710 – 2690 MHz frequency range. Measures made in the Satimo STARGATE 32 anechoic chamber.

2.4. Conclusions

From what is developed in this chapter, it can be concluded that for the presented devices of all four of the applications that are analyzed:

- Most of the devices cover the 4G frequency bands, alongside other frequency bands such as WiFi, Bluetooth or GNSS.
- For **Fleet Management**, the average PCB size is around **80mm x 50mm**.
- For the case of the **modules**, the average PCB size is around **45mm x 35mm**.
- For **OBDs**, the average PCB size is around **55mm x 40mm**.
- For the **IoT devices**, the average PCB size is around **55mm x 50mm**.

Taking into account the frequency bands to cover and the average PCB size of the analyzed devices, the **TRIO mXTEND™** is the most suitable Fractus Antennas (NN) product to use due to its dimensions and the frequency bands that can cover efficiently.

3. EFFICIENCY'S DEPENDANCE ON THE GROUND PLANE LENGTH OF A PCB

3.1. Introduction

In this chapter it is presented a study that has been done for the TRIO mXTEND™ regarding how the efficiency changes depending on the ground plane length.

The followed steps to carry out this study consist in cutting the PCB to the required length, designing the filters and matching network for each case, while measuring the reflection coefficient step-by-step, to finally measure the antenna efficiency.
For all the cases, it is started with the standard PCB for the TRIO mXTEND™ (Figure 10), which is 142mm x 60mm (130mm x 60mm of ground plane).

First, it is soldered the chip antenna component according to the footprint of the antenna.
Later, the micro-coaxial 50Ω transmission line that goes from the end of the matching network to the connector is made and integrated into the PCB.
After that, the filters are designed according to which frequency bands are willing to be optimized. For the case of this project, it is given preference to the LFR (698 – 960 MHz) while not damaging significantly the performance on the HFR (1710 – 2690 MHz).
The next step is designing the matching network step by step, integrating one component at each time and checking that the response, in terms of reflection coefficient, of the last placed component is the desired one.

The function of the filters (Figure 13.a, Figure 13.b) is to optimize the performance of the LFR (698 – 960 MHz) and the HFR (1710 – 2690 MHz).
According to the considered topology for the matching network, the values of the components of the matching network is determined such that each component contributes as exposed in the following lines:

The first component of the matching network, Z_1, is a series inductor to compensate the capacitive impedance of the chip antenna component.
Z_2 and Z_2's function is to achieve a first resonance in the LFR (698 – 960 MHz) by using a shunt inductor and a series capacitor, which have an important effect of the LFR and slightly move the HFR.
After that, Z_4 is placed as a shunt capacitor to bring the HFR closer to the center of the Smith Chart.
Z_5 can be used for fine tuning in case the result from the first four components is not the desired or expected one.

(a)

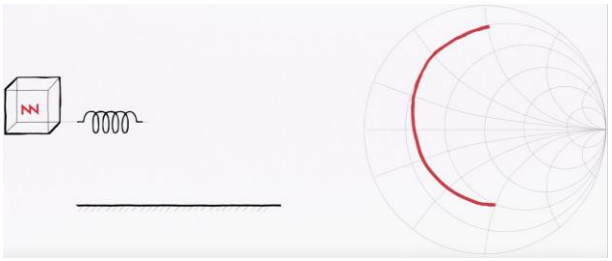

(b)

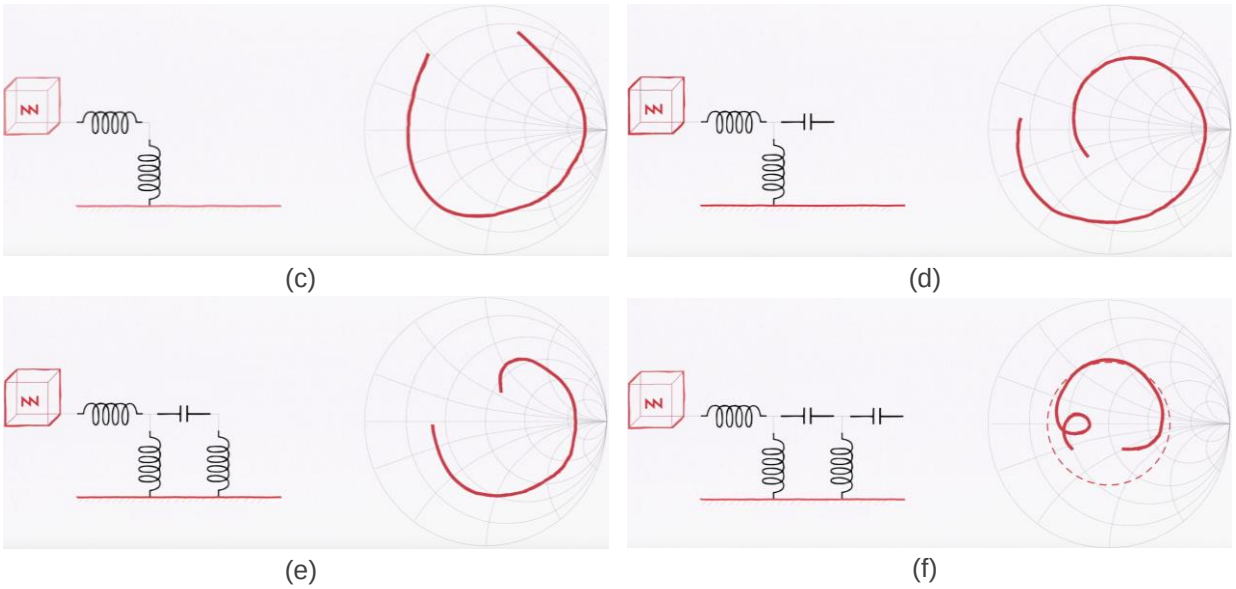

Figure 16 – Starting point (a) and step-by-step contribution of each of the first five components of the matching network, Z_1 (b), Z_2 (c), Z_3 (d), Z_4 (e) and Z_5 (f) for a pentaband solution (824 – 960 MHz; 1710 – 2690 MHz) [36].

Since the objective is to cover a broader bandwidth than the one that the topology in Figure 16 would cover, Z_6 and Z_7 are necessary. The aim of these components, consecutive shunt inductor and capacitor, is to create loops (in the Smith Chart) inside the bands to widen the matched bandwidth.

Finally, a component for fine tuning can be added. Z_8 is typically an inductor and it will allow to move the HFR to matching, while slightly affecting on the LFR.

3.2. 130mm x 60mm platform

In this section it is going to be analyzed the case of using the PCB as it is, considering the 130mm x 60mm of ground plane.

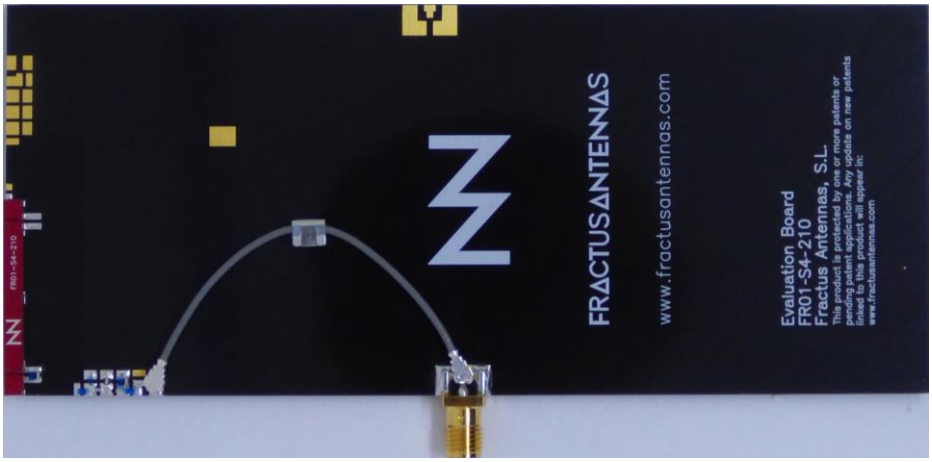

Figure 17 – 130mm x 60mm ground plane final solution.

3.2.1. Matching Network

In Table 6 is presented the matching network for the 130mm x 60mm case (Figure 17). It has been used the same as in 2.3.2.

Component	Value	Part number
F1	15 nH	LQW18AN15NG80
F2	0.3 pF	GJM1555C1HR30WB01
F3	Empty	-
F4	Empty	-
Z1	2.2 nH	LQW18AN2N2C80
Z2	8.6 nH	LQW15AN8N6G80
Z3	2.2 pF	GJM1555C1H2R2WB01
Z4	1 pF	GJM1555C1H1R0WB01
Z5	0Ω	-
Z6	10 nH	LQW18AN10NG80
Z7	0.36 pF	GJM1555C1HR36WB01
Z8	3 nH	LQW18AN3N0C80

Table 6 – Matching network values for the 130mm x 60mm of ground plane case.

3.2.2. Reflection coefficient

In this section is shown the reflection coefficient of the 130mm x 60mm (Figure 17). It is achieved an S_{11} (dB) < -6dB all along the ranges of interest.

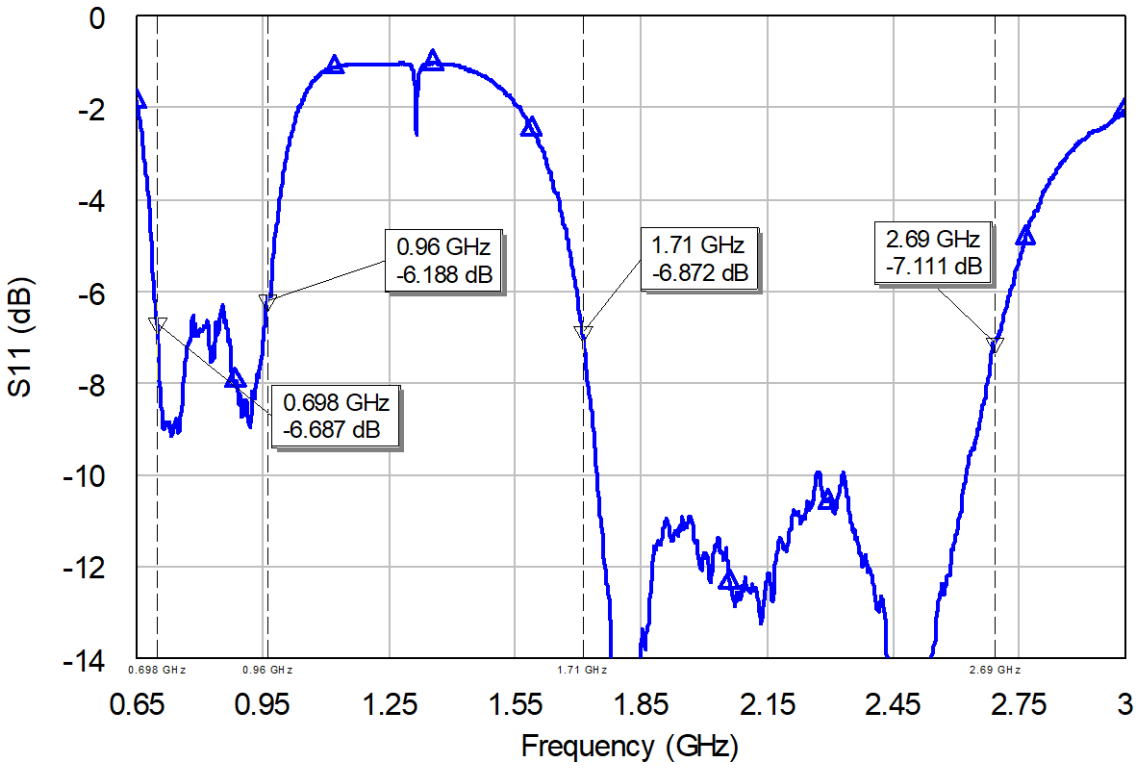

Figure 18 – Reflection coefficient for the 130mm x 60mm of ground plane case.

3.2.3. Efficiency (%)

The antenna and radiation efficiency are presented in this section (Figure 19) for the 130mm x 60mm. It is achieved a 60.1% of antenna efficiency on the LFR and a 74.3% on the HFR.

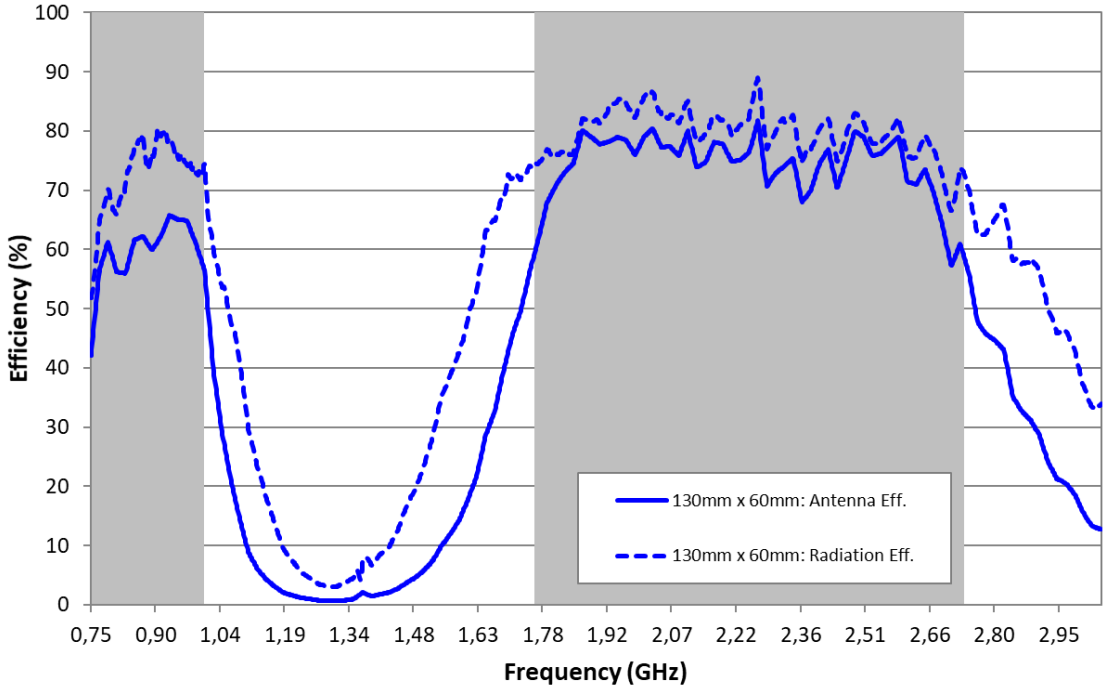

Figure 19 – Antenna and Radiation Efficiency (%) for the 130mm x 60mm of ground plane case.

	LFR (698 – 960 MHz)					HFR (1710 – 2690 MHz)				
Ground Plane dimensions (mm x mm)	**$\eta_{a\ 698\ MHz}$**	**$\eta_{a\ 960\ MHz}$**	**Min**	**Max**	**Av. η_a**	**$\eta_{a\ 1710\ MHz}$**	**$\eta_{a\ 2690\ MHz}$**	**Min**	**Max**	**Av. η_a**
130mm x 60mm	42.0	56.5	42.0	65.7	**60.1**	59.1	58.5	57.3	8.8	**74.3**

Table 7 – Antenna efficiency (%) for the 130mm x 60mm ground plane case.

3.3. 80mm x 60mm platform

The case exposed in the current section considers the PCB cut to 80mm x 60mm.

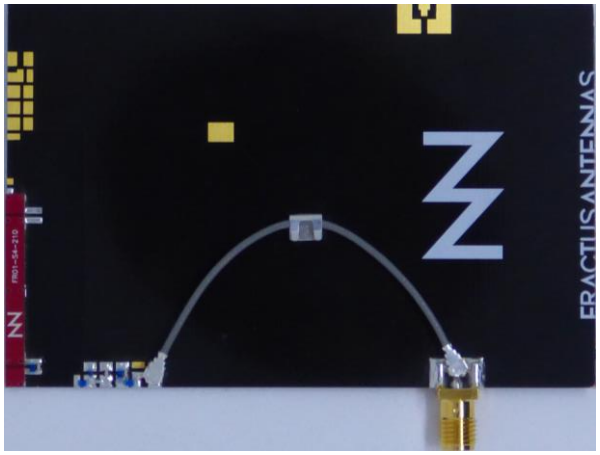

Figure 20 – 80mm x 60mm ground plane final solution.

3.3.1. Matching Network

In Table 8 is presented the matching network for the 80mm x 60mm case. It is decided to short-circuit the second filter (F3, F4) since it allows to use all the chip antenna component and improves the performance in terms of efficiency. From now on, the second filter will be short-circuited for all the cases.

Component	Value	Part number
F1	13 nH	LQW18AN13NG80
F2	0.4 pF	GJM1555C1HR40WB01
F3	0Ω	-
F4	Empty	-
Z1	3.7 nH	LQW15AN3N7G80
Z2	9.1 nH	LQW18AN9N1G80
Z3	2.2 pF	GJM1555C1H2R2WB01
Z4	0.9 pF	GJM1555C1HR90WB01
Z5	0Ω	-
Z6	13 nH	LQW18AN13NG80
Z7	0.36 pF	GJM1555C1HR36WB01
Z8	1.8 nH	LQW15AN1N8C00

Table 8 – Matching network values for the 80mm x 60mm of ground plane case.

3.3.2. Reflection coefficient

The obtained S_{11} (dB) (Figure 21) for the 80mm x 60mm case (Figure 20) on the LFR is around -4dB in all the region, while the HFR keeps a similar performance as for 130mm x 60mm (3.2.2).

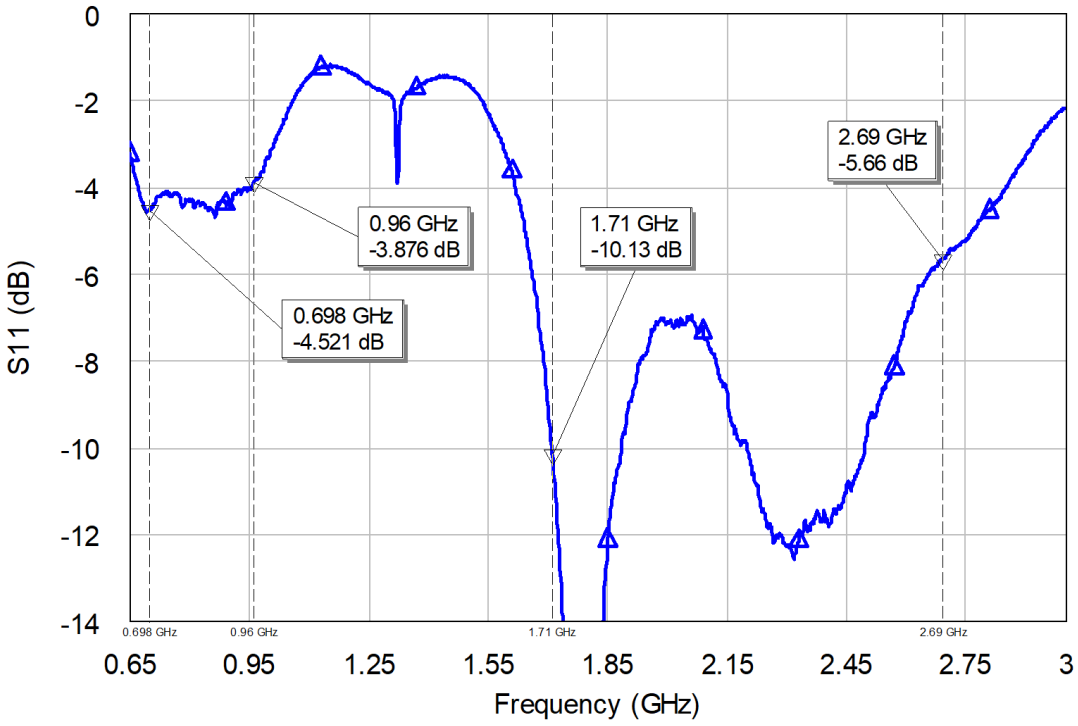

Figure 21 – Reflection coefficient for the 80mm x 60mm of ground plane case.

3.3.3. Efficiency (%)

The achieved antenna efficiency on the LFR is 31.2%, while the HFR offers 62.5%.

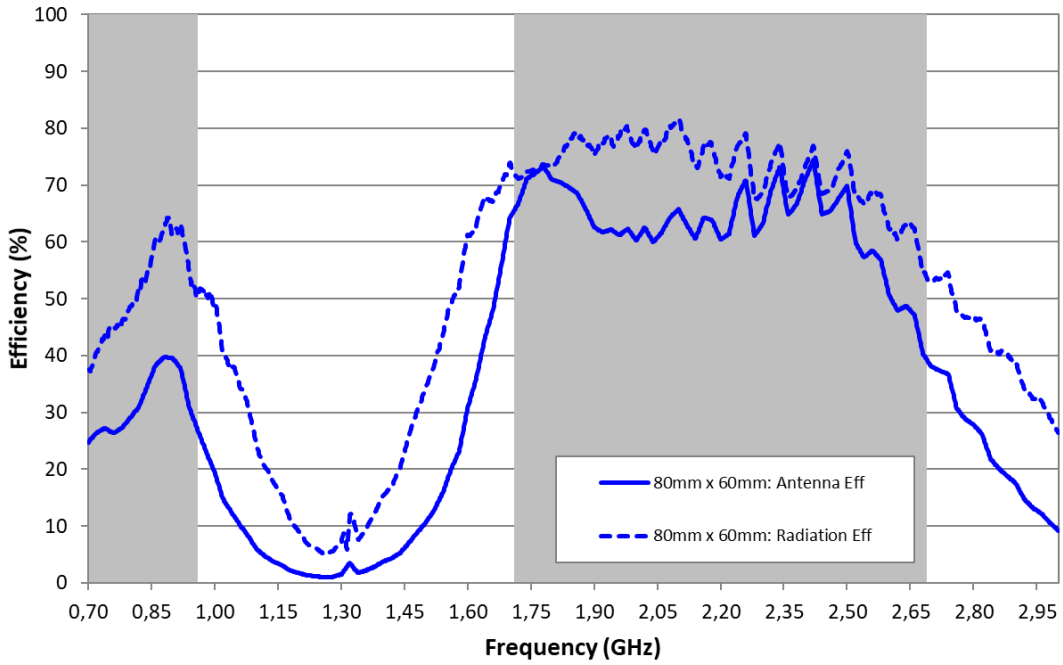

Figure 22 – Antenna and Radiation Efficiency (%) for the 80mm x 60mm of ground plane case.

	LFR (698 – 960 MHz)					HFR (1710 – 2690 MHz)				
Ground Plane dimensions (mm x mm)	**$\eta_{a\ 698\ MHz}$**	**$\eta_{a\ 960\ MHz}$**	**Min**	**Max**	**Av. η_a**	**$\eta_{a\ 1710\ MHz}$**	**$\eta_{a\ 2690\ MHz}$**	**Min**	**Max**	**Av. η_a**
80mm x 60mm	24.2	25.5	24.2	37.9	**31.2**	63.0	38.0	38.0	72.7	**62.5**

Table 9 – Antenna efficiency (%) for the 80mm x 60mm ground plane case.

3.4. 60mm x 60mm platform

The case exposed in the current section considers the PCB cut to 60mm x 60mm, for which a coaxial cable had to be made.

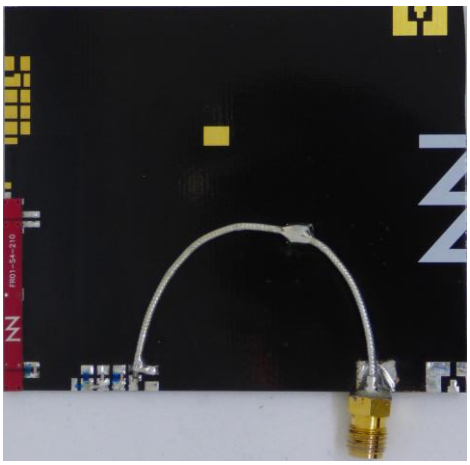

Figure 23 – 60mm x 60mm ground plane final solution.

3.4.1. Matching Network

In Table 10 is presented the matching network for the 60mm x 60mm case (Figure 23).

Component	Value	Part number
F1	12 nH	LQW18AN12NG10
F2	0.5 pF	GJM1555C1HR50WB01
F3	0Ω	-
F4	Empty	-
Z1	2.2 nH	LQW15AN2N2G80
Z2	8.4 nH	LQW18AN8N4G80
Z3	2.2 pF	GJM1555C1H2R2WB01
Z4	1 pF	GJM1555C1H1R0WB01
Z5	0Ω	-
Z6	10 nH	LQW18AN10NG80
Z7	0.4 pF	GJM1555C1HR40WB01
Z8	0Ω	-

Table 10 – Matching network values for the 60mm x 60mm of ground plane case.

3.4.2. Reflection coefficient

In this section is shown the reflection coefficient (Figure 24) of the 60mm x 60mm case (Figure 23). The S_{11} (dB) on the LFR is between -2.7dB and -4dB, while on the HFR it still presents a deep matching in the band but on the upper edge of the band it suffers a decrease in terms of matching.

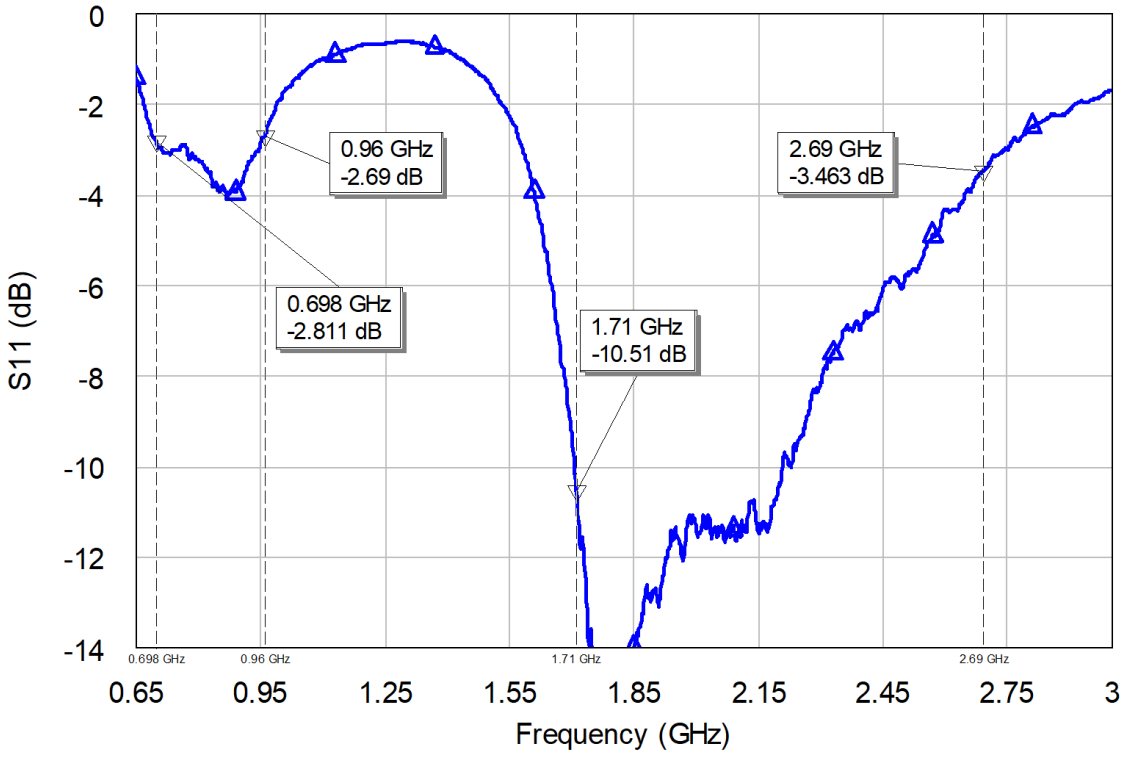

Figure 24 – Reflection coefficient for the 60mm x 60mm of ground plane case.

3.4.3. Efficiency (%)

The antenna efficiency value keeps its order on the HFR (68.9%). On the LFR, it drops to 25.0%. This reduction is due to a lesser excitation of the ground plane mode [12].

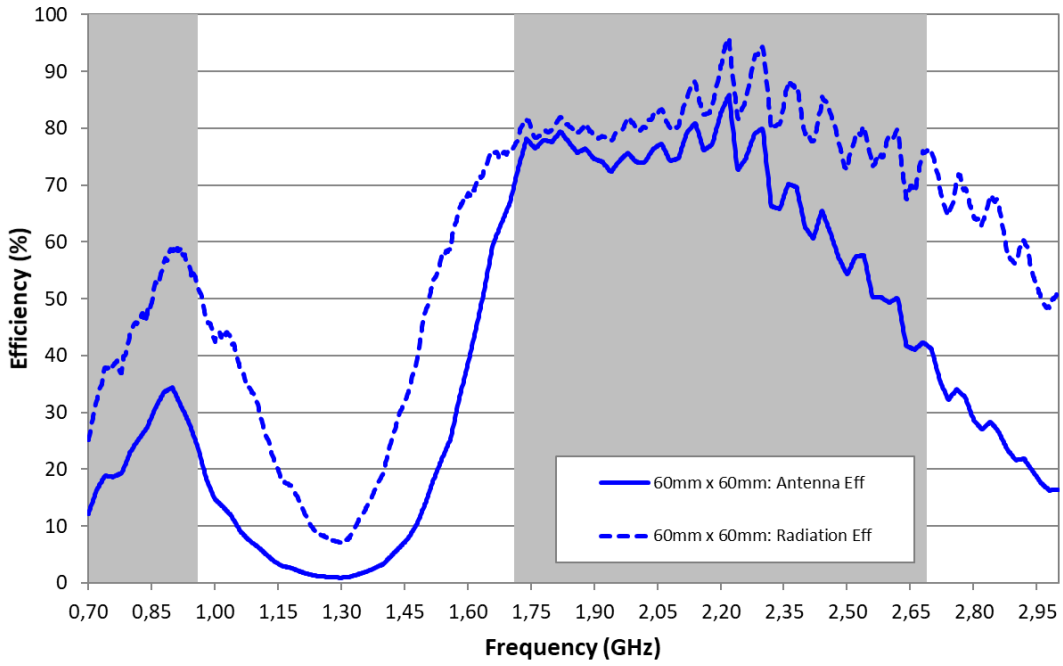

Figure 25 – Antenna and Radiation Efficiency (%) for the 60mm x 60mm of ground plane case.

	LFR (698 – 960 MHz)					HFR (1710 – 2690 MHz)				
Ground Plane dimensions (mm x mm)	**$\eta_{a\ 698\ MHz}$**	**$\eta_{a\ 960\ MHz}$**	**Min**	**Max**	**Av. η_a**	**$\eta_{a\ 1710\ MHz}$**	**$\eta_{a\ 2690\ MHz}$**	**Min**	**Max**	**Av. η_a**
60mm x 60mm	12.2	24.0	12.0	34.4	**25.0**	69.9	41.8	41.1	85.9	**68.9**

Table 11 – Antenna efficiency (%) for the 60mm x 60mm ground plane case.

3.5. 40mm x 60mm platform

The case exposed in the current section considers the PCB cut to 40mm x 60mm, for which a coaxial cable had to be made.

Figure 26 – 40mm x 60mm ground plane final solution.

3.5.1. Matching Network

In Table 12 is presented the matching network for the 60mm x 60mm case (Figure 26).

Component	Value	Part number
F1	12 nH	LQW18AN12NG10
F2	0.5 pF	GJM1555C1HR50WB01
F3	0Ω	-
F4	Empty	-
Z1	2.2 nH	LQW15AN2N2G80
Z2	8.4 nH	LQW18AN8N4G80
Z3	2.2 pF	GJM1555C1H2R2WB01
Z4	0.7 pF	GJM1555C1HR70WB01
Z5	0Ω	-
Z6	10 nH	LQW18AN10NG80
Z7	0.3 pF	GJM1555C1HR30WB01
Z8	2.2 nH	LQW15AN2N2G80

Table 12 – Matching network values for the 40mm x 60mm of ground plane case.

3.5.2. Reflection coefficient

In this section is shown the 40mm x 60mm case's (Figure 26) reflection coefficient (Figure 27). On the LFR it is obtained an S_{11} (dB) < -2dB along the region, while on the HFR the S_{11} is lower than -4dB.

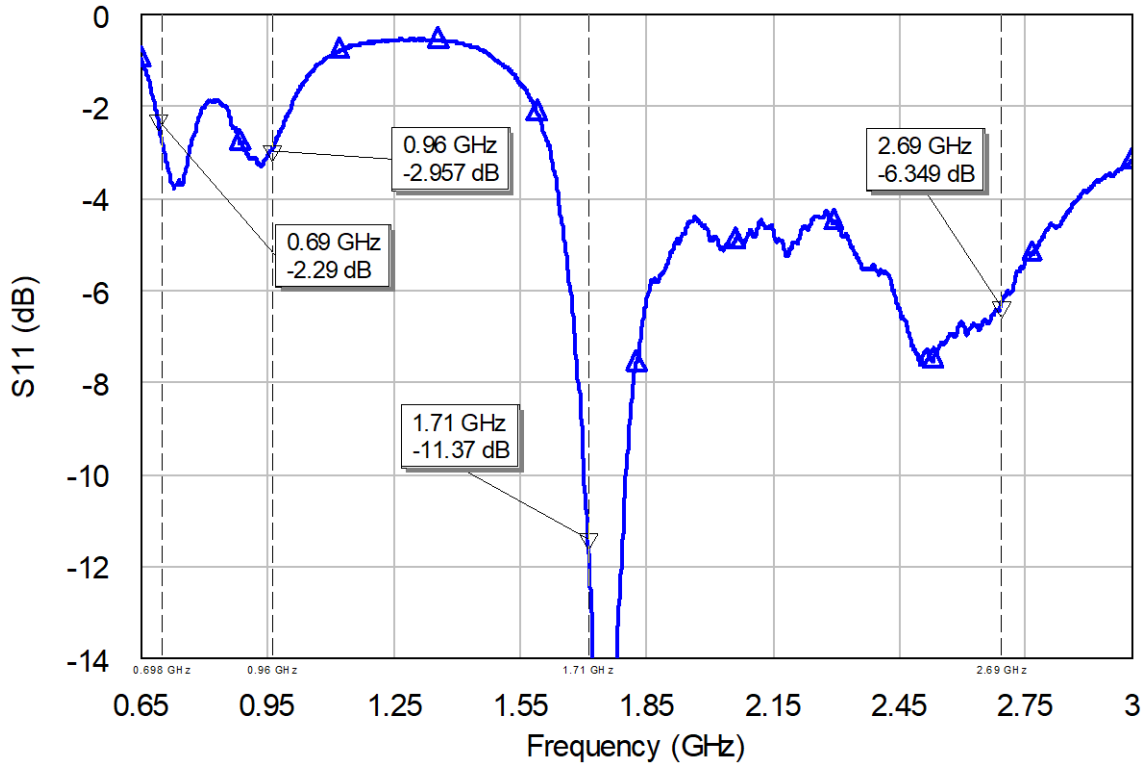

Figure 27 – Reflection coefficient for the 40mm x 60mm of ground plane case.

3.5.3. Efficiency (%)

The obtained antenna efficiency on the LFR drops to 17.8%. Moreover, on the HFR it is noticed that the performance starts to decrease (58.8%).

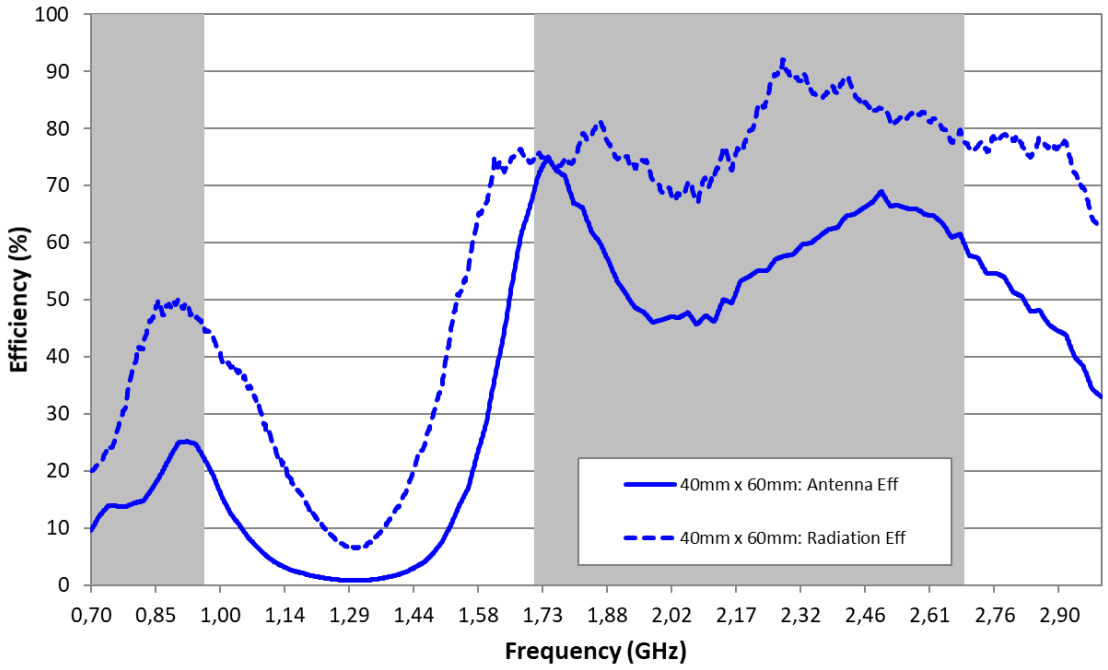

Figure 28 – Antenna and Radiation Efficiency (%) for the 40mm x 60mm of ground plane case.

	LFR (698 – 960 MHz)					HFR (1710 – 2690 MHz)				
Ground Plane dimensions (mm x mm)	**$\eta_{a\ 698\ MHz}$**	**$\eta_{a\ 960\ MHz}$**	**Min**	**Max**	**Av. η_a**	**$\eta_{a\ 1710\ MHz}$**	**$\eta_{a\ 2690\ MHz}$**	**Min**	**Max**	**Av. η_a**
40mm x 60mm	9.6	22.1	9.6	25.1	**17.8**	69.2	59.6	45.7	74.9	**58.8**

Table 13 – Antenna efficiency (%) for the 40mm x 60mm ground plane case.

3.6. Conclusions

It has been analyzed the effect of the ground plane length on the antenna efficiency (Figure 29 and Table 14) on the prototypes shown in Figure 30 concluding that the impact is more pronounced for the LFR whereas HFR remains practically the same.
This information is very helpful for wireless device designers to determine the minimum PCB size a device should have in order to attain a certain efficiency value.

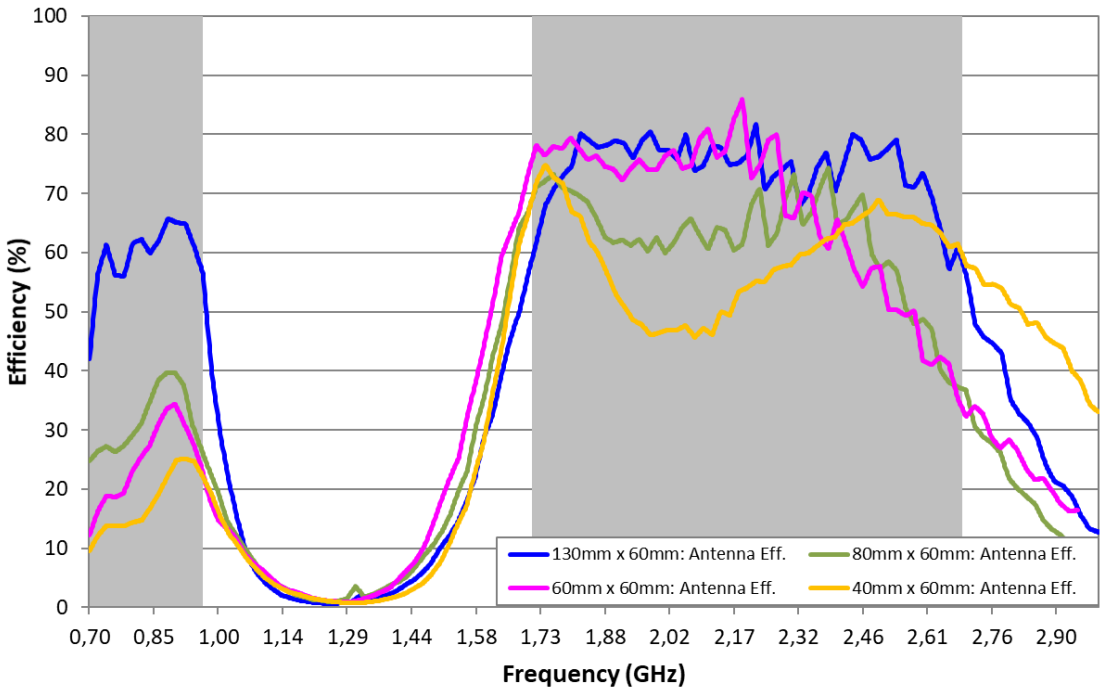

Figure 29 – Antenna and Radiation Efficiency (%) comparison of the different considered ground plane lengths.

	LFR (698 – 960 MHz)					HFR (1710 – 2690 MHz)				
Ground Plane dimensions (mm x mm)	**$\eta_{a\ 698\ MHz}$**	**$\eta_{a\ 960\ MHz}$**	**Min**	**Max**	**Av. η_a**	**$\eta_{a\ 1710\ MHz}$**	**$\eta_{a\ 2690\ MHz}$**	**Min**	**Max**	**Av. η_a**
130mm x 60mm	42.0	56.5	42.0	65.7	**60.1**	59.1	58.5	57.3	8.8	**74.3**
80mm x 60mm	24.2	25.5	24.2	37.9	**31.2**	63.0	38.0	38.0	72.7	**62.5**
60mm x 60mm	12.2	24.0	12.0	34.4	**25.0**	69.9	41.8	41.1	85.9	**68.9**
40mm x 60mm	9.6	22.1	9.6	25.1	**17.8**	69.2	59.6	45.7	74.9	**58.8**

Table 14 – Antenna efficiency (%) for all the analyzed cases.

By analyzing the antenna efficiency drop in dB (Table 15) it can be concluded that the length of the ground plane affects more to the LFR than the HFR. While the LFR suffers a drop of 0.5-0.6dB/10mm, the HFR almost suffers no changes (Table 16).

	LFR (698 – 960 MHz)	HFR (1710 – 2690 MHz)
Efficiency drop (dB)	Av. η_a	Av. η_a
130mm to 80mm	2.9	0.8
130mm to 60mm	3.8	0.3
130mm to 40mm	5.3	1.0

Table 15 – Antenna efficiency drop for all the analyzed cases (referenced to the 130mm x 60mm case).

	LFR (698 – 960 MHz)	HFR (1710 – 2690 MHz)
Efficiency drop (dB/10mm)	Av. η_a	Av. η_a
130mm to 80mm	0.6	0.1
130mm to 60mm	0.5	0.1
130mm to 40mm	0.6	0.1

Table 16 – Antenna efficiency drop (dB/10mm) for all the analyzed cases (referenced to the 130mm x 60mm case).

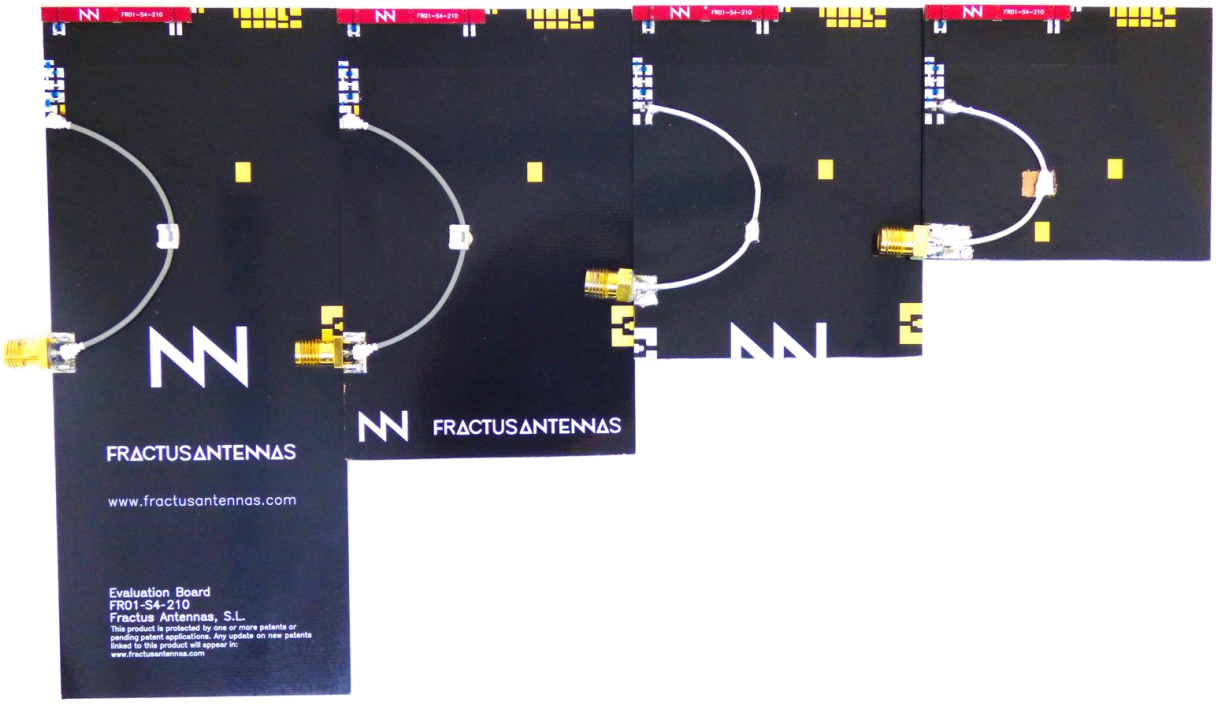

Figure 30 – Ground length experiment PCBs. From left to right, 130mm x 60mm, 80mm x 60mm, 60mm x 60mm and 40mm x 60mm..

4. ACTIVE SOLUTION FOR FLEET MANAGEMENT SIZE

4.1. Introduction

This chapter explores a technique that consists in implementing several selective matching networks for the sake of improving the efficiency of the system. To do so, it will be considered the Fleet Management devices' size (80mm x 50mm) that has been extracted from the benchmarking made on Chapter 2.
The two regions to cover, LFR (698 – 960 MHz) and HFR (1710 – 2690 MHz), are divided in several narrower bands and each of those bands will be covered by a dedicated matching network.

When implementing this technique in a real device, besides the bank of matching networks, two switches will be needed [27]:
The first switch should be located between the feeding line and the start of the matching network to allow the division of the single feeding into the different paths that will lead to the matching networks, and the second one should be placed between the end of the matching network and the I/O port of the RF module to re-unify the paths of the different matching networks into a single transmission line.
Those switches introduce losses. After a search and analysis of the datasheets of several RF switches, it will be considered along this project that the insertion losses that each of the switches introduces is 0.3dB.

The LFR has been split in 5 bands, which are: 698 – 748 MHz, 746 – 803 MHz, 791-849 MHz, 824 – 894 MHz and 880-960 MHz. On the other hand, the HFR is treated as a single band and will be matched with a single matching network. The regions have been divided in that way due to the difficulty of matching and the efficiency that could be reached with a broadband matching network in such small platforms, especially on the LFR.

The matching networks that will be designed for the LFR will be two-component matching networks to keep a good compromise between matching and efficiency (each component adds losses besides its contribution to matching).

First, an electromagnetic simulation will be done, implementing a broadband matching network that covers the full bandwidth to obtain the efficiencies that will be taken as reference to improve when considering the active solution.
After that, the analysis of the active solution will be carried out on the same simulated model to have an order of magnitude of the efficiencies that can be obtained, the needed topology for the matching network and quantify how much can the efficiency be improved implementing the analyzed technique respect to the broadband matching network for the passive solution.
Finally, prototypes will be mounted and measured taking into account the active solution.

4.2. Electromagnetic Analysis

In this section, the results of the electromagnetic analysis of the solution presented in this chapter will be shown. To do so, the CST electromagnetic simulator is used.

A model with an 80mm x 50mm PCB is prepared to simulate. In this PCB it is integrated the chip antenna used along this project and the ports for the filters and the components of the matching network are created.

First, a multiband matching network for the created model will be designed to obtain the efficiency values to which the ones obtained from the active solution will be referenced.
After that, it is proceeded to design the matching networks for each of the bands.

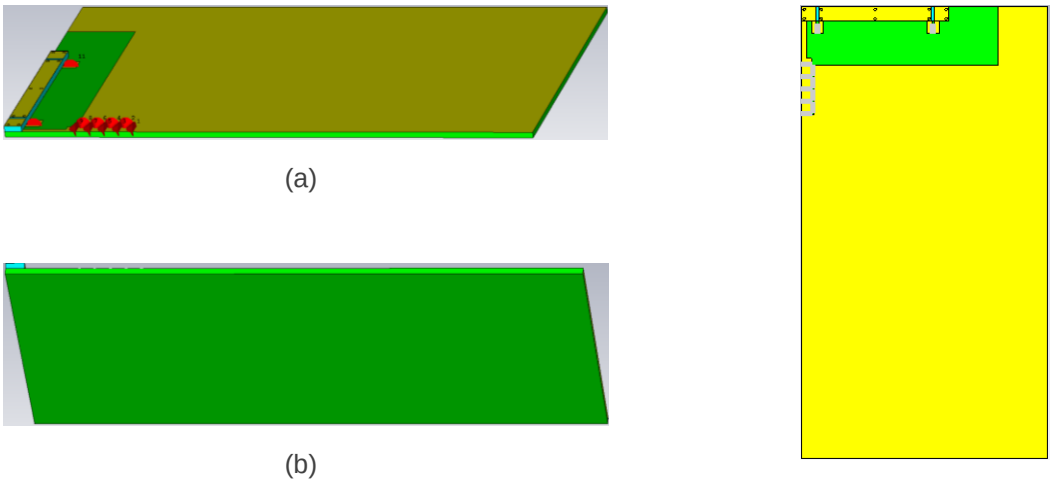

(a)

(b)

(c)

Figure 31 – CST model for the simulations of Fleet Management PCB size. Top (a, c) and bottom (b) views. FR4 substrate is 1mm thickness, ε_r=4.15, tanδ=0.012.

For all the matching networks designed for the simulated model, the same filters, shown in Table 17, are used.

Component		Value	P/N
Filter 1	F1	12 nH	LQW18AN12NG10
	F2	0.4 pF	GJM1555C1HR40WB01
Filter 2	F3	0Ω	-
	F4	Empty	-

Table 17 – Filters for the Electromagnetic Analysis of the Fleet Management PCB size.

4.2.1. Passive solution

In this section is designed the passive solution, including a multiband matching network to cover 698 – 960 MHz and 1710 – 2690 MHz. The obtained reflection coefficient and efficiency from the designed matching network are presented.

4.2.1.1. Matching network

The resulting Matching Network for the passive solution is shown in Table 18.

Component	Value	P/N
Z1	4.2 nH	LQW15AN4N2G80
Z2	10 nH	LQW18AN10NG80
Z3	0.5 pF	GJM1555C1HR50WB01
Z4	0.8 pF	GJM1555C1HR80WB01
Z5	0Ω	-
Z6	15 nH	LQW18AN15NG80
Z7	0.4 pF	GJM1555C1HR40WB01
Z8	2.2 nH	LQW15AN2N2G80

Table 18 – Broadband Matching Network values for the Fleet Management PCB size.

4.2.1.2. Reflection coefficient

The multiband matching network offers an S_{11} (dB) < -2dB on the LFR, while on the HFR it is obtained S_{11} (dB) < -4.8dB (Figure 32).

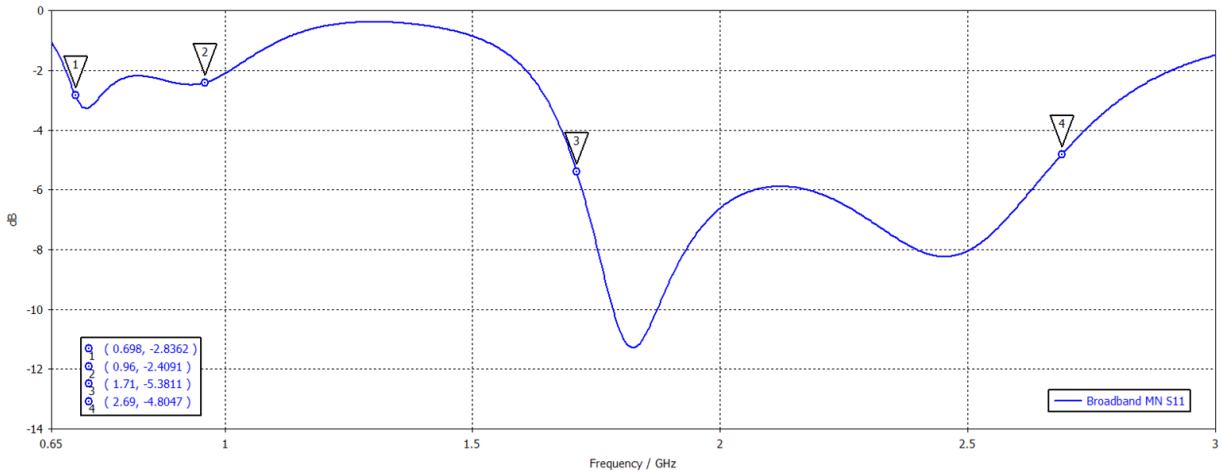

Figure 32 – Reflection coefficient for the Broadband Matching Network in Table 18.

4.2.1.3. Efficiency (%)

The antenna efficiency on the LFR is 30.2% and 69.0% on the HFR.

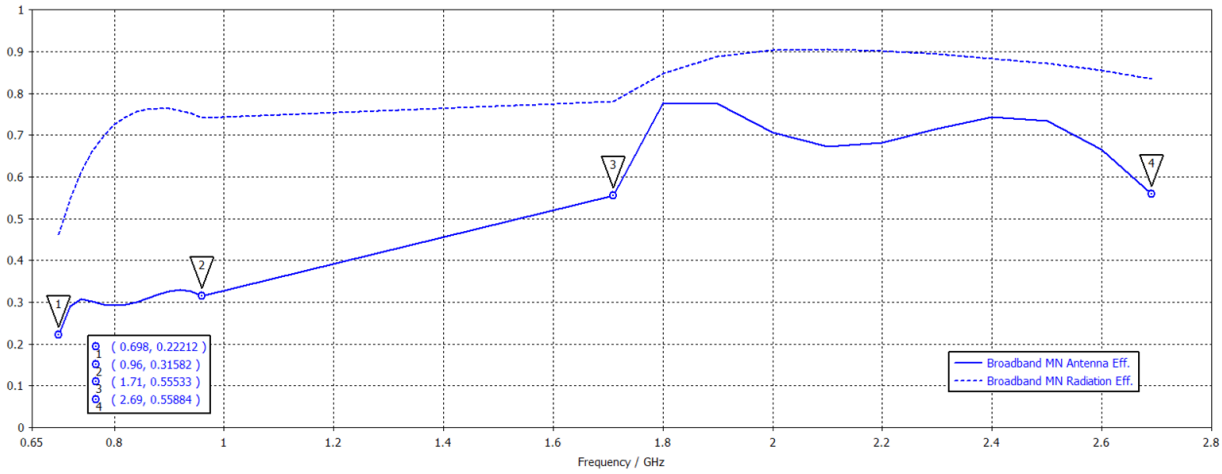

Figure 33 – Antenna and Radiation Efficiency (%) for the Broadband Matching Network (Table 18).

	LFR (698 – 960 MHz)					HFR (1710 – 2690 MHz)				
Frequency range of interest	**$\eta_{a\ 698\ MHz}$**	**$\eta_{a\ 960\ MHz}$**	**Min**	**Max**	**Av. η_a**	**$\eta_{a\ 1710\ MHz}$**	**$\eta_{a\ 2690\ MHz}$**	**Min**	**Max**	**Av. η_a**
Broadband MN	22.2	31.6	22.2	33.0	**30.2**	55.5	55.9	55.5	77.8	**69.0**

Table 19 – Antenna efficiency (%) for the simulated Broadband Matching Network (Table 18).

4.2.2. 698 – 748 MHz

In this section is designed the first dedicated matching network. This will cover 698 – 748 MHz. The obtained reflection coefficient and efficiency from the designed matching network are presented.

4.2.2.1. Matching network

The two-component matching network for 698 – 748 MHz is shown in Table 20. In this case and the following ones, the matching network is very simple, since there is no need to match a multiband frequency region, but a single band.

Component	Value	P/N
Z1	30 nH	LQW18AN30NG80
Z2	7.6 pF	GJM1555C1H7R6WB01
Z3	0Ω	-
Z4	Empty	-
Z5	0Ω	-
Z6	Empty	-
Z7	Empty	-
Z8	0Ω	-

Table 20 – Matching Network values for covering 698 – 748 MHz with the Fleet Management PCB size.

4.2.2.2. Reflection coefficient

The corresponding reflection coefficient for 698 – 748 MHz is shown in Figure 34. It is achieved a deep matching, keeping the edges at -3.9dB and -1.8dB.

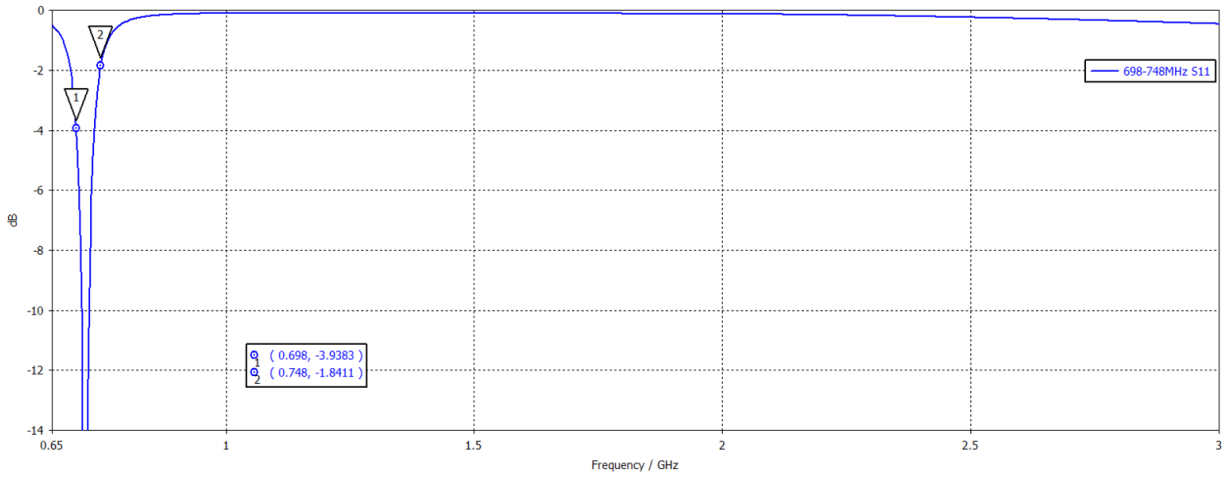

Figure 34 – Reflection coefficient for the Broadband Matching Network in Table 20.

4.2.2.3. Efficiency (%)

The antenna efficiency obtained for 698 – 748 MHz is 31.6%.

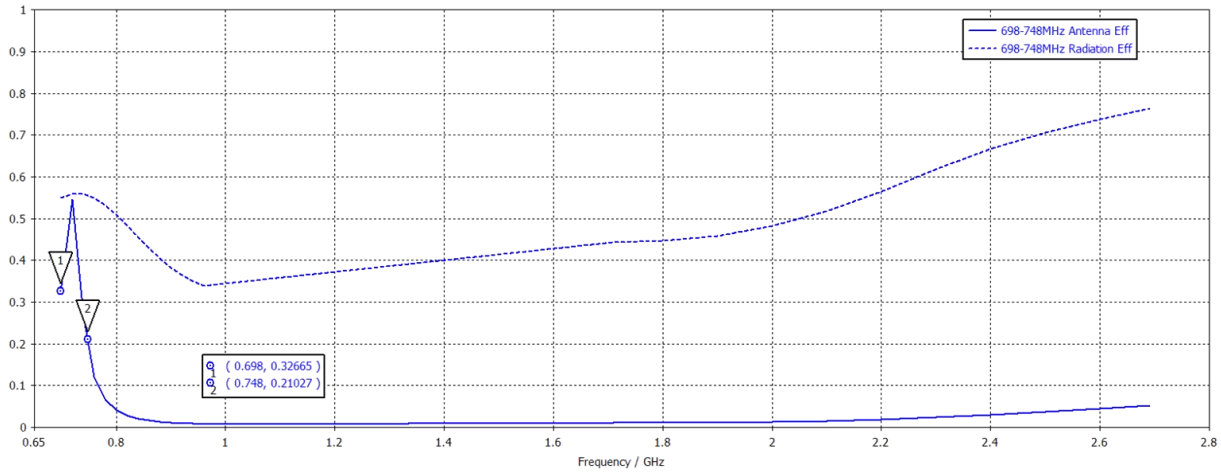

Figure 35 – Antenna and Radiation Efficiency (%) for the 698 – 749MHz Matching Network (Table 20).

	Antenna Efficiency (%)				
Frequency range of interest	**η_{a} 698 MHz**	**η_{a} 748 MHz**	**Min**	**Max**	**Av. η_{a}**
698 – 748 MHz MN	32.7	21.0	21.0	54.7	**31.6**

Table 21 – Antenna efficiency (%) for the simulated Matching Network for 698 – 748 MHz (Table 20).

4.2.3. 746 – 803 MHz

The second dedicated matching network is presented in this section, along with its reflection coefficient and efficiency. The covered range of frequencies is 746 – 803 MHz.

4.2.3.1. Matching network

The two-component matching network for 746 – 803 MHz is shown in Table 22.

Component	Value	P/N
Z1	23 nH	LQW18AN23NG80
Z2	5.0 pF	GJM1555C1H5R0WB01
Z3	0Ω	-
Z4	Empty	-
Z5	0Ω	-
Z6	Empty	-
Z7	Empty	-
Z8	0Ω	-

Table 22 – Matching Network values for covering 746 – 803 MHz with the Fleet Management PCB size.

4.2.3.2. Reflection coefficient

The obtained reflection coefficient is presented in Figure 36. A -10dB matching is almost achieved, while the edges of the band are at -4.2B and -3.3dB.

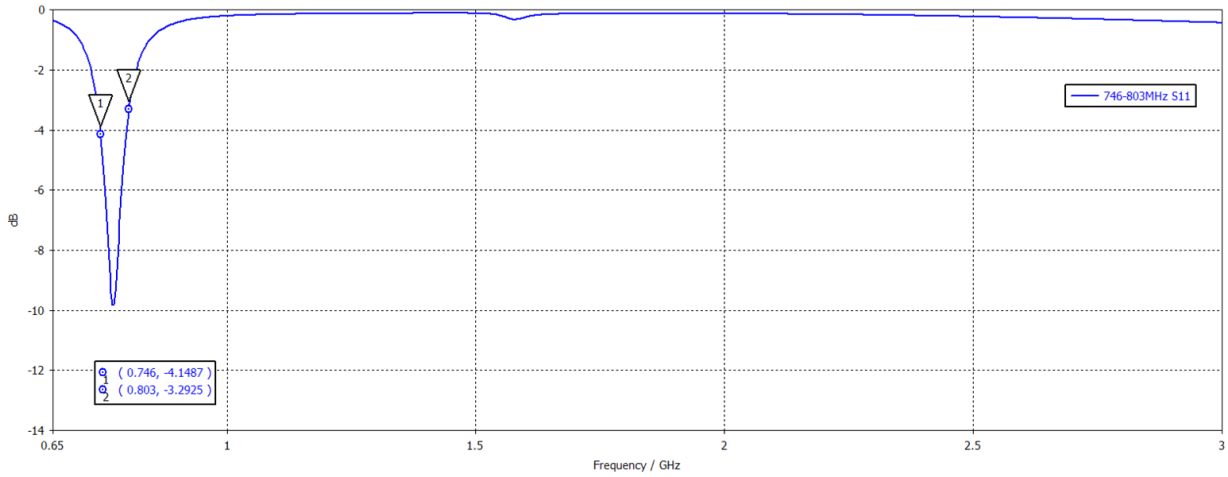

Figure 36 – Reflection coefficient for the Matching Network for 746 – 803 MHz in Table 22.

4.2.3.3. Efficiency (%)

From the matching network shown in Table 22 it is obtained an antenna efficiency of 45.9% for 746 – 803 MHz.

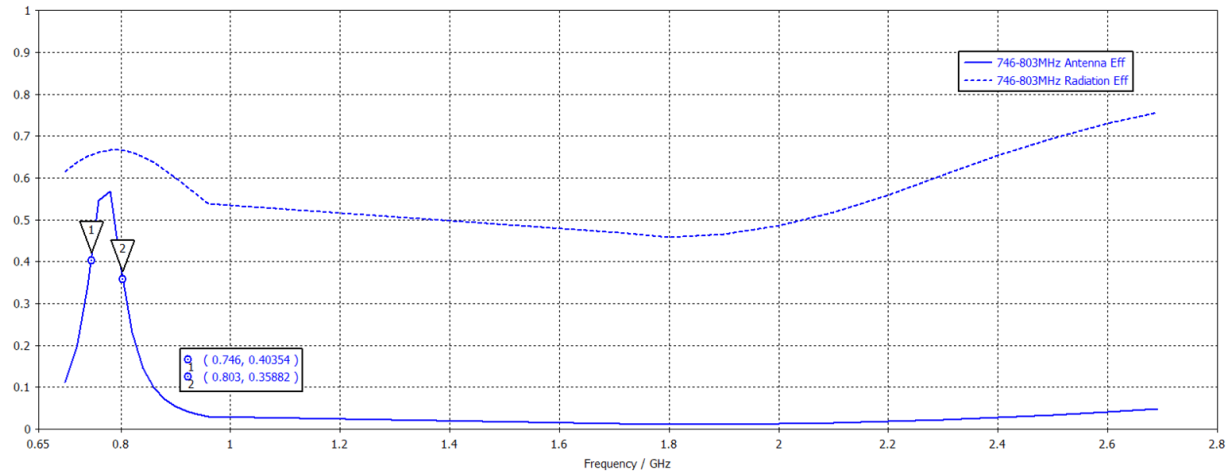

Figure 37 – Antenna and Radiation Efficiency (%) for the 746 – 803 MHz Matching Network (Table 22).

	Antenna Efficiency (%)				
Frequency range of interest	**η_{a} 746 MHz**	**η_{a} 803 MHz**	**Min**	**Max**	**Av. η_{a}**
746 – 803 MHz MN	40.4	35.9	35.9	56.8	**45.9**

Table 23 – Antenna efficiency (%) for the simulated Matching Network for 746 – 803 MHz (Table 22).

4.2.4. 791 – 849 MHz

The dedicated matching for 791 – 849 MHz is presented in this section, with its corresponding reflection coefficient and efficiency.

4.2.4.1. Matching network

The matching network made of two components is presented in Table 24.

Component	Value	P/N
Z1	17 nH	LQW18AN17NG80
Z2	5.2 pF	GJM1555C1H5R2WB01
Z3	0Ω	-
Z4	Empty	-
Z5	0Ω	-
Z6	Empty	-
Z7	Empty	-
Z8	0Ω	-

Table 24 – Matching Network values for covering 791 – 849 MHz with the Fleet Management PCB size.

4.2.4.2. Reflection coefficient

The corresponding reflection coefficient presents band edges at around -4dB and a deep matching in the center of the band.

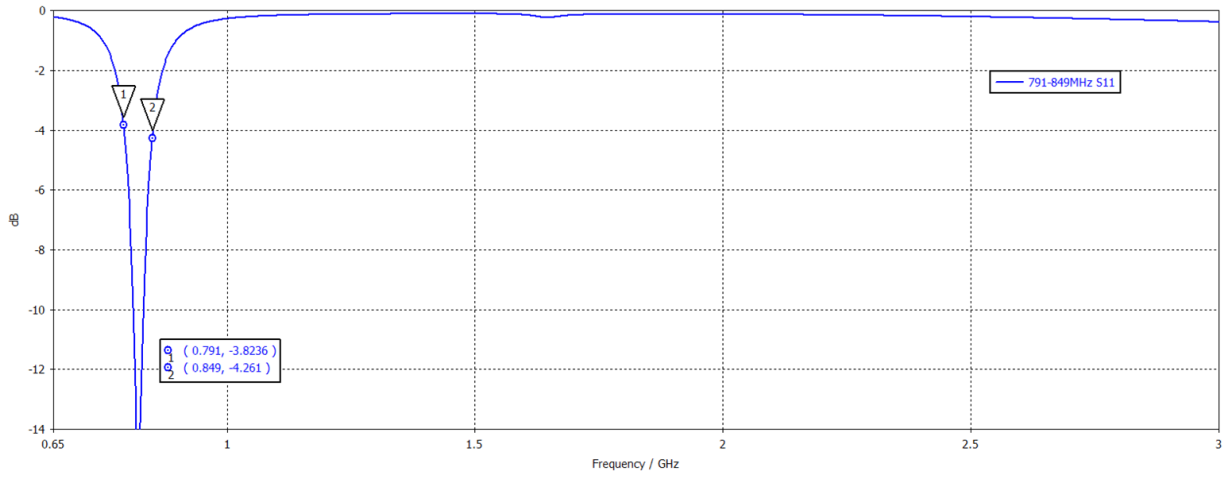

Figure 38 – Reflection coefficient for the Matching Network for 791 – 849 MHz in Table 24.

4.2.4.3. Efficiency (%)

The obtained efficiency for the 791 – 849 MHz band with the two-component matching network is 53.2%.

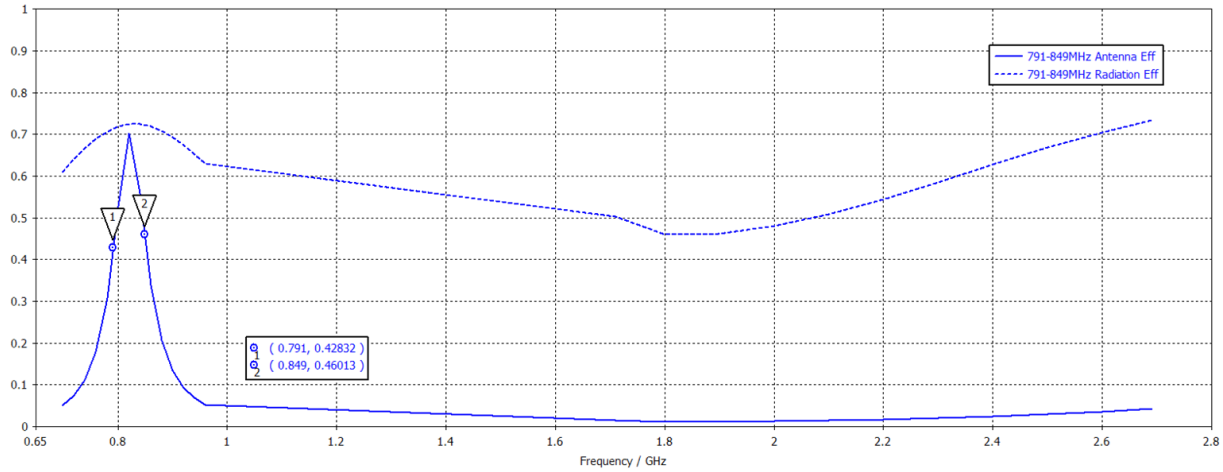

Figure 39 – Antenna and Radiation Efficiency (%) for the 791 – 849 MHz Matching Network (Table 24).

	Antenna Efficiency (%)				
Frequency range of interest	η_{a} 791 MHz	η_{a} 849 MHz	Min	Max	Av. η_{a}
791 – 849 MHz MN	42.8	46.9	42.8	70.3	**53.2**

Table 25 – Antenna efficiency (%) for the simulated Matching Network for 791 – 849 MHz (Table 24).

4.2.5. 824 – 894 MHz

In this section is designed the matching network that will cover 824 – 894 MHz. The obtained reflection coefficient and efficiency from the designed matching network are presented.

4.2.5.1. Matching network

The two-component dedicated matching network for 824 – 894 MHz is shown in Table 26.

Component	Value	P/N
Z1	14 nH	LQW15AN14NG80
Z2	3.9 pF	GJM1555C1H3R9WB01
Z3	0Ω	-
Z4	Empty	-
Z5	0Ω	-
Z6	Empty	-
Z7	Empty	-
Z8	0Ω	-

Table 26 – Matching Network values for covering 824 – 894 MHz with the Fleet Management PCB size.

4.2.5.2. Reflection coefficient

For this case, it is reached a deep matching of -10dB in the center of the band, while the edges are below -4dB.

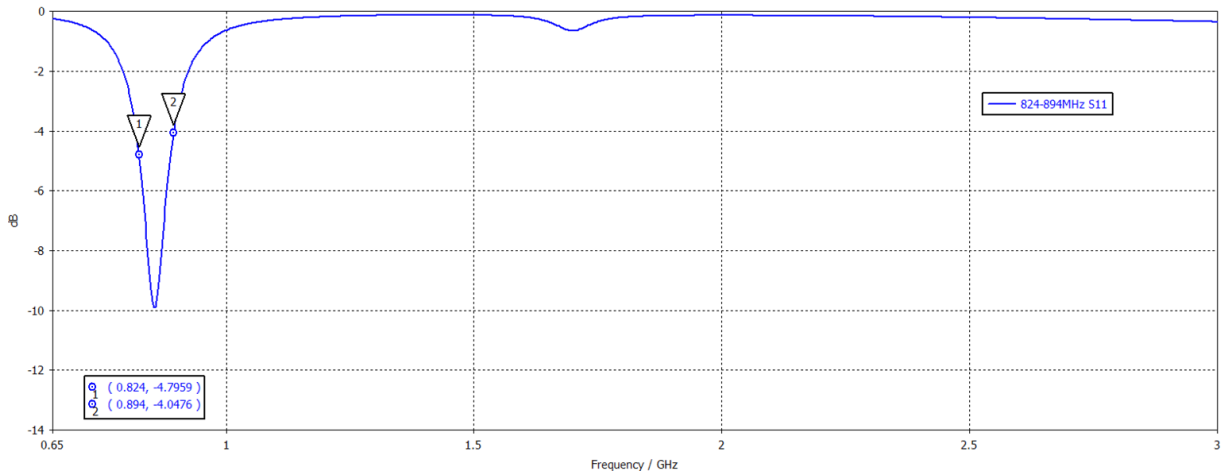

Figure 40 – Reflection coefficient for the Matching Network for 824 – 894 MHz in Table 26.

4.2.5.3. Efficiency (%)

The antenna efficiency reached with the matching network for 824 – 894 MHz is 52.3%.

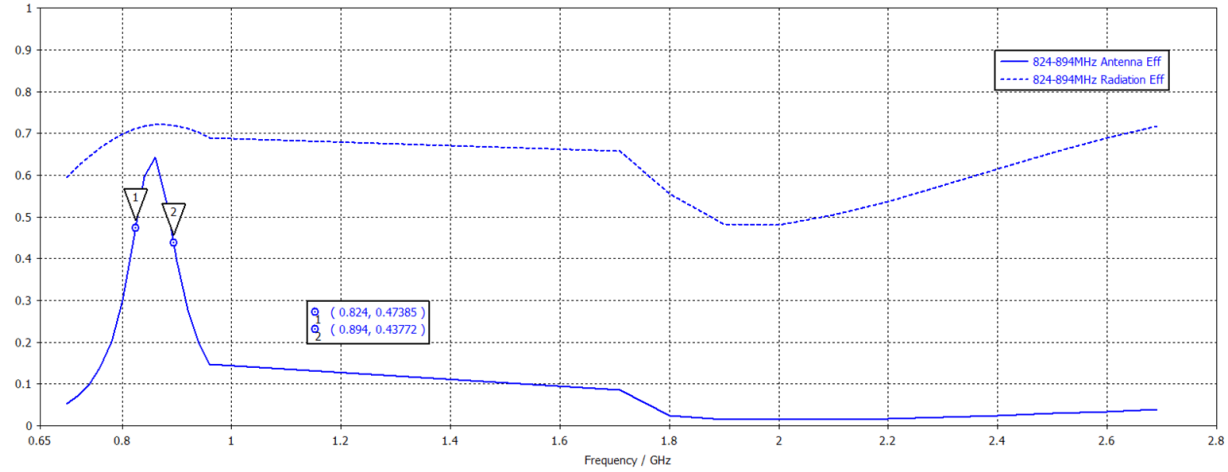

Figure 41 – Antenna and Radiation Efficiency (%) for the 824 – 894 MHz Matching Network (Table 26).

	Antenna Efficiency (%)				
Frequency range of interest	**η_{a} 824 MHz**	**η_{a} 894 MHz**	**Min**	**Max**	**Av. η_{a}**
824 – 894 MHz MN	47.4	43.8	43.8	64.4	**52.3**

Table 27 – Antenna efficiency (%) for the simulated Matching Network 824 – 894 MHz (Table 26).

4.2.6. 880 – 960 MHz

In this section is presented the last selective matching network for the LFR, which covers 880 – 960 MHz. Alongside, its corresponding reflection coefficient and efficiency are presented.

4.2.6.1. Matching network

For 880 – 960 MHz, the designed matching network is presented in Table 28.

Component	Value	P/N
Z1	7.2 nH	LQW18AN7N2C80
Z2	3.5 pF	GJM1555C1H3R5WB01
Z3	0Ω	-
Z4	Empty	-
Z5	0Ω	-
Z6	Empty	-
Z7	Empty	-
Z8	0Ω	-

Table 28 – Matching Network values for covering 880 – 960 MHz with the Fleet Management PCB size.

4.2.6.2. Reflection coefficient

The obtained S_{11} for this band presents edges below -4dB and a deep matching of -11dB.

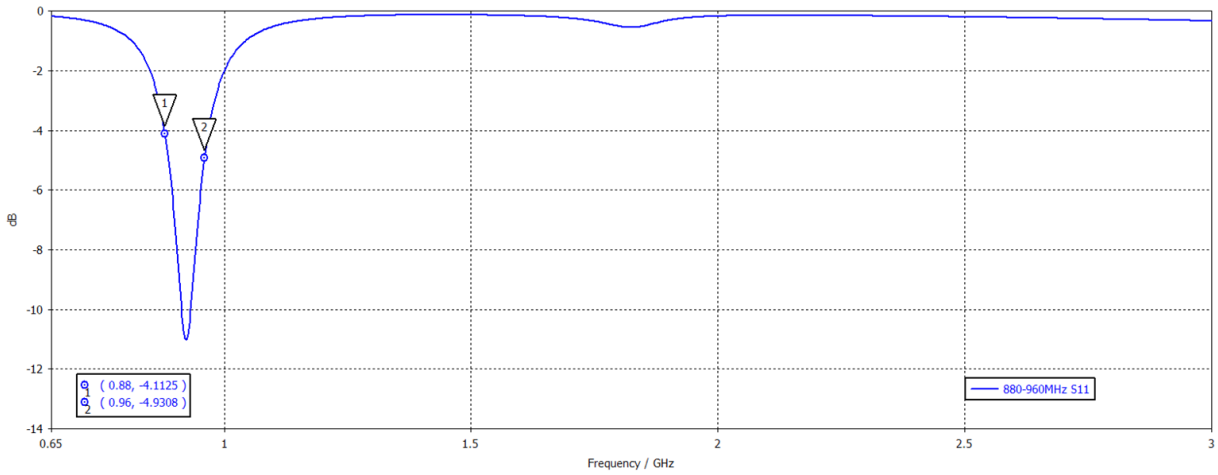

Figure 42 – Reflection coefficient for the Matching Network for 880 – 960 MHz in Table 28.

4.2.6.3. Efficiency (%)

The antenna efficiency obtained for this band presents a minimum of almost 50% and an average of 62.3%.

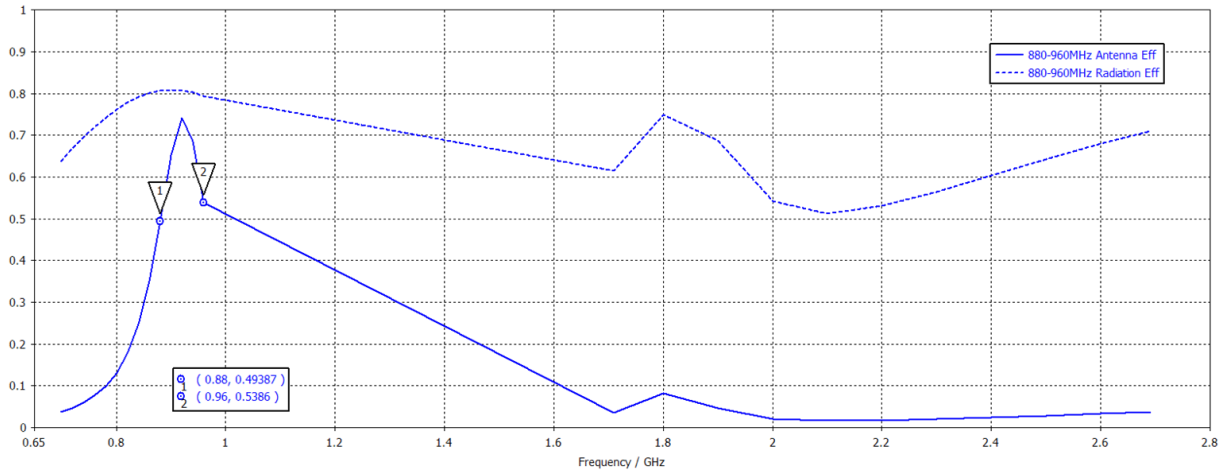

Figure 43 – Antenna and Radiation Efficiency (%) for the 880 – 960 MHz Matching Network (Table 28).

	Antenna Efficiency (%)				
Frequency range of interest	$\eta_{a\ 880\ MHz}$	$\eta_{a\ 960\ MHz}$	Min	Max	Av. η_a
880 – 960 MHz MN	49.4	53.9	49.4	74.2	**62.3**

Table 29 – Antenna efficiency (%) for the simulated Matching Network 880 – 960 MHz (Table 28).

4.2.7. 1710 – 2690 MHz

The selective matching network for the HFR, 1710 – 2690 MHz, is presented in this section together with its reflection coefficient and efficiency.

4.2.7.1. Matching network

The designed matching network for the HFR consists of 3 components.

Component	Value	P/N
Z1	3.5 nH	LQW15AN3N5G80
Z2	0.4 pF	GJM1555C1HR40WB01
Z3	3.8 nH	LQW15AN3N8G80
Z4	Empty	-
Z5	0Ω	-
Z6	Empty	-
Z7	Empty	-
Z8	0Ω	-

Table 30 – Matching Network values for covering 1710 – 2690 MHz with the Fleet Management PCB size.

4.2.7.2. Reflection coefficient

The matching network exposed in Table 30 offers an S_{11} (dB) < -4dB along all the band, with a good matching below -6dB in almost all the band.

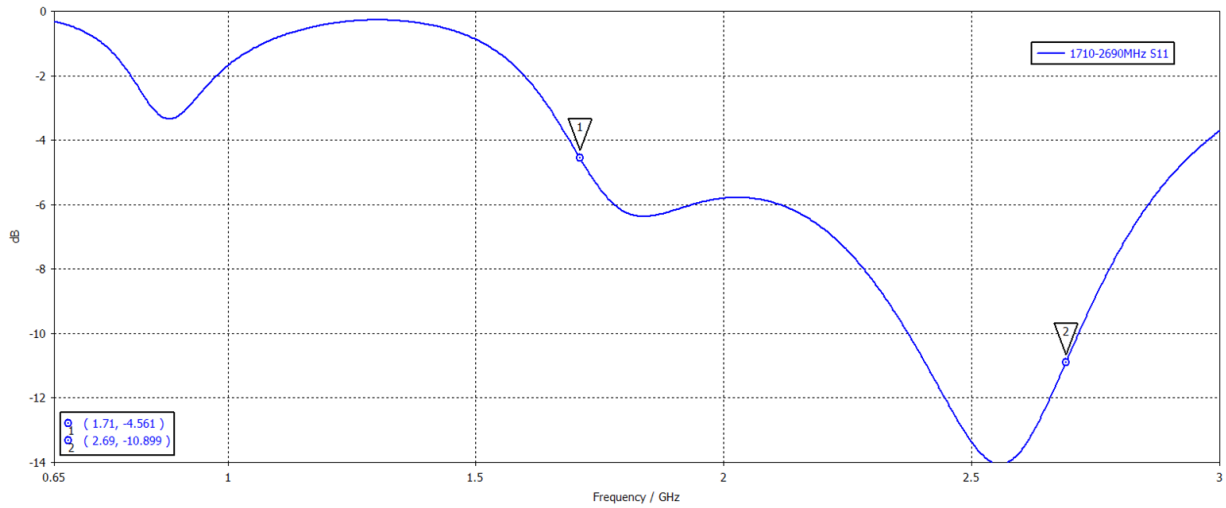

Figure 44 – Reflection coefficient for the Matching Network for 1710 – 2690 MHz in Table 30.

4.2.7.3. Efficiency (%)

The antenna efficiency for this case is 74.2%, with a minimum value of 50.8%.

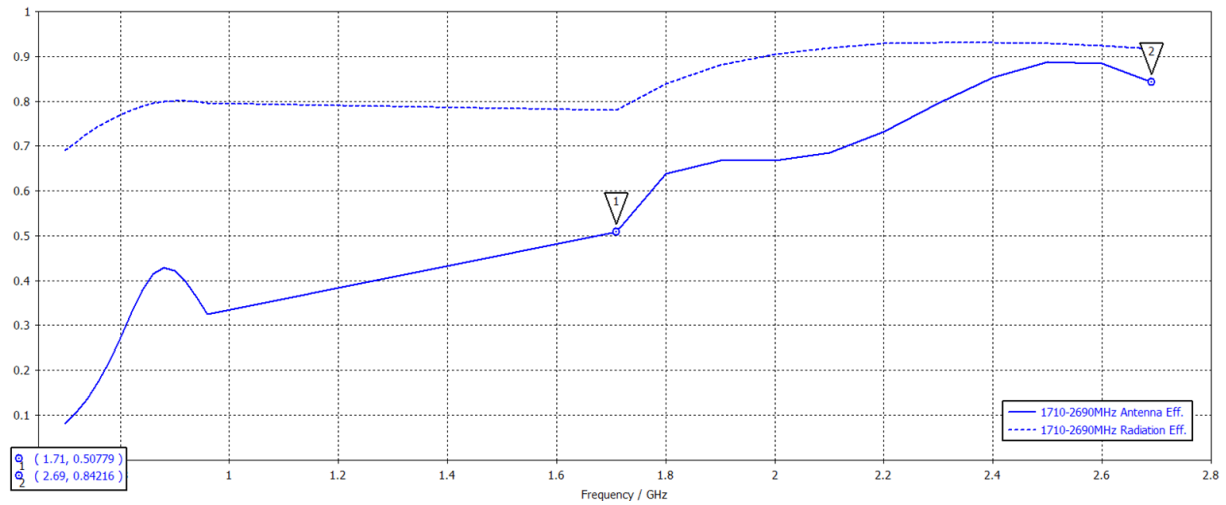

Figure 45 – Antenna and Radiation Efficiency (%) for the 1710 – 2690 MHz Matching Network (Table 30).

	Antenna Efficiency (%)				
Frequency range of interest	**η_a 1710 MHz**	**η_a 2690 MHz**	**Min**	**Max**	**Av. η_a**
1710 – 2690 MHz MN	50.8	84.2	50.8	88.7	**74.2**

Table 31 – Antenna efficiency (%) for the simulated Matching Network for 1710 – 2690 MHz (Table 30).

4.2.8. Summary

There is a significant improvement of the active solution respect to the classical passive solution (Figure 46).

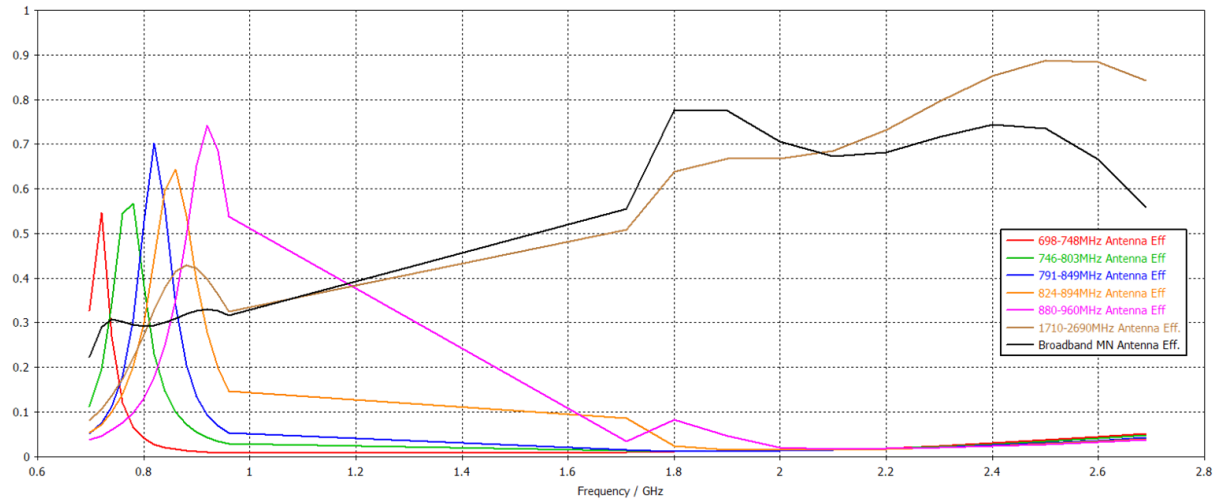

Figure 46 – Antenna Efficiency (%) of the Multiband Matching Network vs the active solution of the simulations for the Fleet Management size.

The active matching networks offer much better efficiencies than the broadband matching network for all the frequency bands of the LFR (698 – 960 MHz).
On the other hand, the HFR (1710 – 2690 MHz) is slightly better for the case of using the broadband matching network.

The slight decrease in the efficiency for the HFR (3.8% less in active solution than in passive) is not significative respect to the improvement that it presents for the LFR (average around the 55.0% for the active solution, while for the passive solution is 30.0%).

4.3. Prototyping and Measurements

After seeing the significant improvement that can be obtained by implementing the active solution in the electromagnetic analysis, it is decided to move on to the prototyping stage to validate the electromagnetic analysis.

The filters to implement are shown in Table 32. Those filters allow to have an optimal balance between the performance of the HFR and the losses that are introduced to the LFR.

The designed matching networks for all the LFR bands and the HFR will consist of two components, since it offers the optimal compromise between matching and efficiency, maximizing the latter.

Component		Value	P/N
Filter 1	F1	12 nH	LQW18AN12NG10
	F2	0.4 pF	GJM1555C1HR40WB01
Filter 2	F3	0Ω	-
	F4	Empty	-

Table 32 – Filter component values for the active solution of the Fleet Management PCB size prototype.

The resulting prototype is shown in Figure 47.

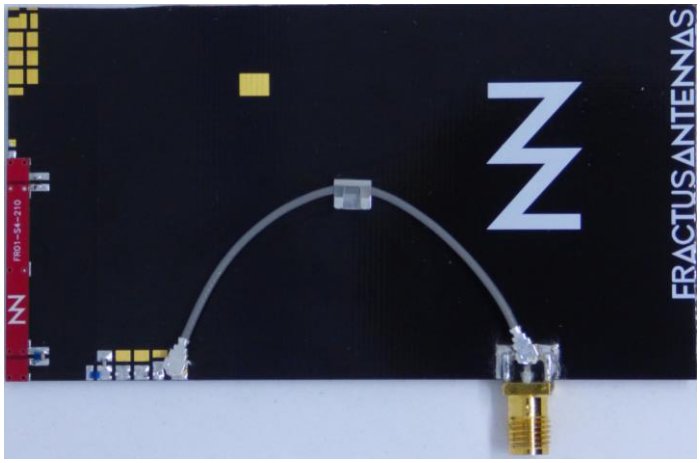

Figure 47 – 80mm x 50mm Fleet Management PCB prototype.

4.3.1. 698 – 748 MHz

4.3.1.1. Matching network

The two-components matching network for 698 – 748 MHz, consisting in a series and a shunt inductor, is presented in Table 33.

Component	Value	P/N
Z1	20 nH	LQW18AN20NG00
Z2	12 nH	LQW18AN12NG10
Z3	0Ω	-
Z4	Empty	-
Z5	0Ω	-
Z6	Empty	-
Z7	Empty	-
Z8	0Ω	-

Table 33 – Measured Matching Network values for 698 – 748 MHz of the Fleet Management PCB size prototype.

4.3.1.2. Reflection coefficient

With that matching network, it is achieved a deep matching in the center of the band, while keeping the edges of the band around -6dB.

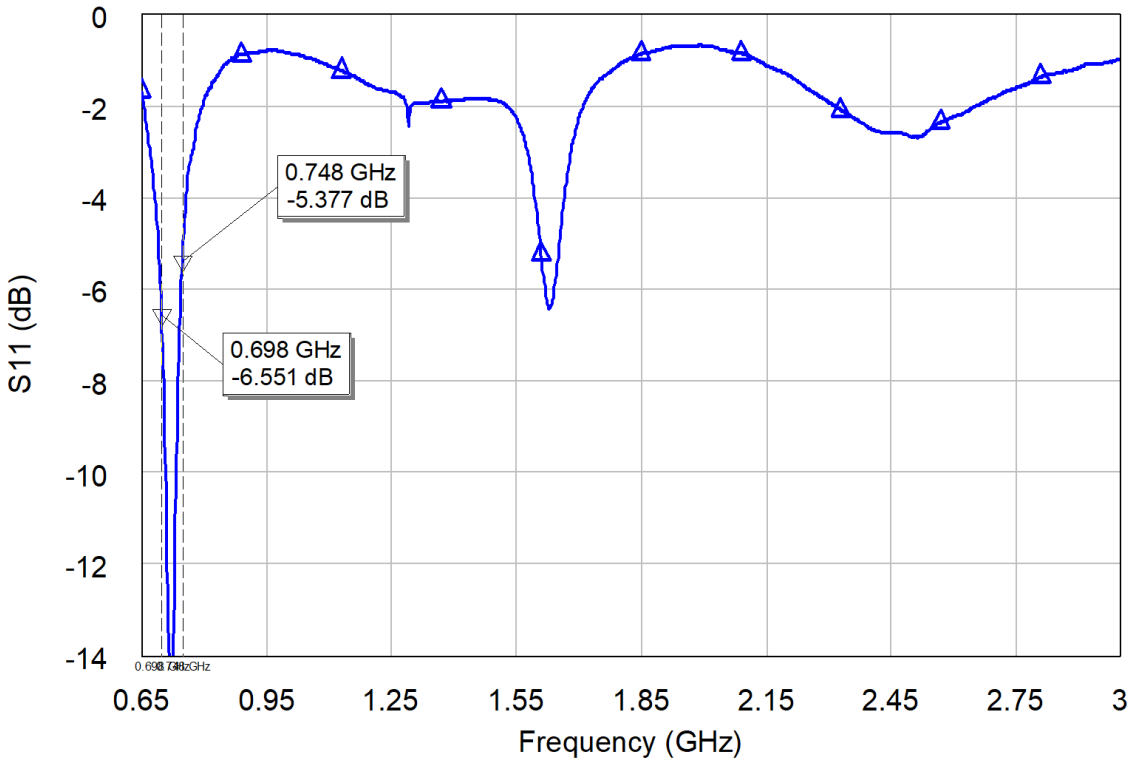

Figure 48 – Reflection coefficient for the Matching Network for 698 – 748 MHz in Table 33.

4.3.1.3. Efficiency (%)

The antenna efficiency achieved for this band is 39.5%.

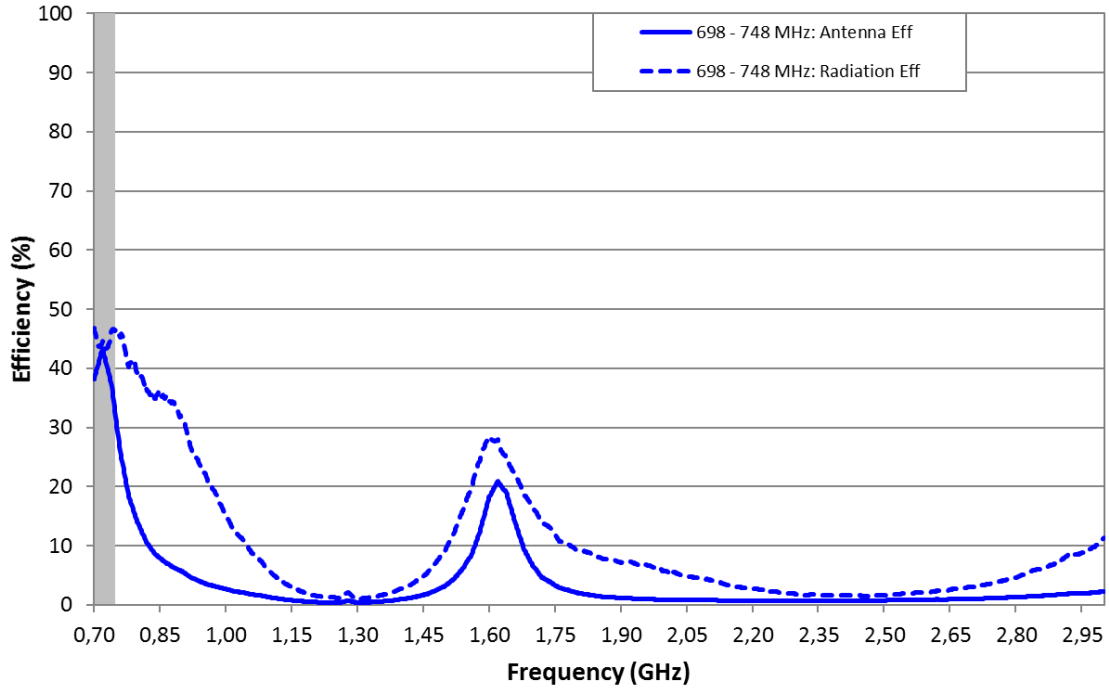

Figure 49 – Antenna and Radiation Efficiency (%) for the Matching Network (Table 33).

	Antenna Efficiency (%)				
Frequency range of interest	$\eta_{a\ 698\ MHz}$	$\eta_{a\ 748\ MHz}$	Min	Max	Av. η_a
698 – 748 MHz MN	38.1	32.7	32.7	43.3	**39.5**

Table 34 – Antenna efficiency (%) for the measured Matching Network for 698 – 748 MHz (Table 33) on the prototype shown in Figure 47.

4.3.2. 746 – 803 MHz

4.3.2.1. Matching network

For 746 – 803 MHz, the designed matching network is also formed by a series and a shunt inductor (Table 35).

Component	Value	P/N
Z1	13 nH	LQW18AN13NG80
Z2	12 nH	LQW18AN12NG10
Z3	0Ω	-
Z4	Empty	-
Z5	0Ω	-
Z6	Empty	-
Z7	Empty	-
Z8	0Ω	-

Table 35 – Measured Matching Network values for 746 – 803 MHz of the Fleet Management PCB size prototype.

4.3.2.2. Reflection coefficient

The obtained reflection coefficient is S_{11} (dB) < -6dB along 746 – 803 MHz, with deep matching in the center of the band. There is also a non-desired resonance close to the lower edge of the HFR (1710 – 2690 MHz) with a deep matching.

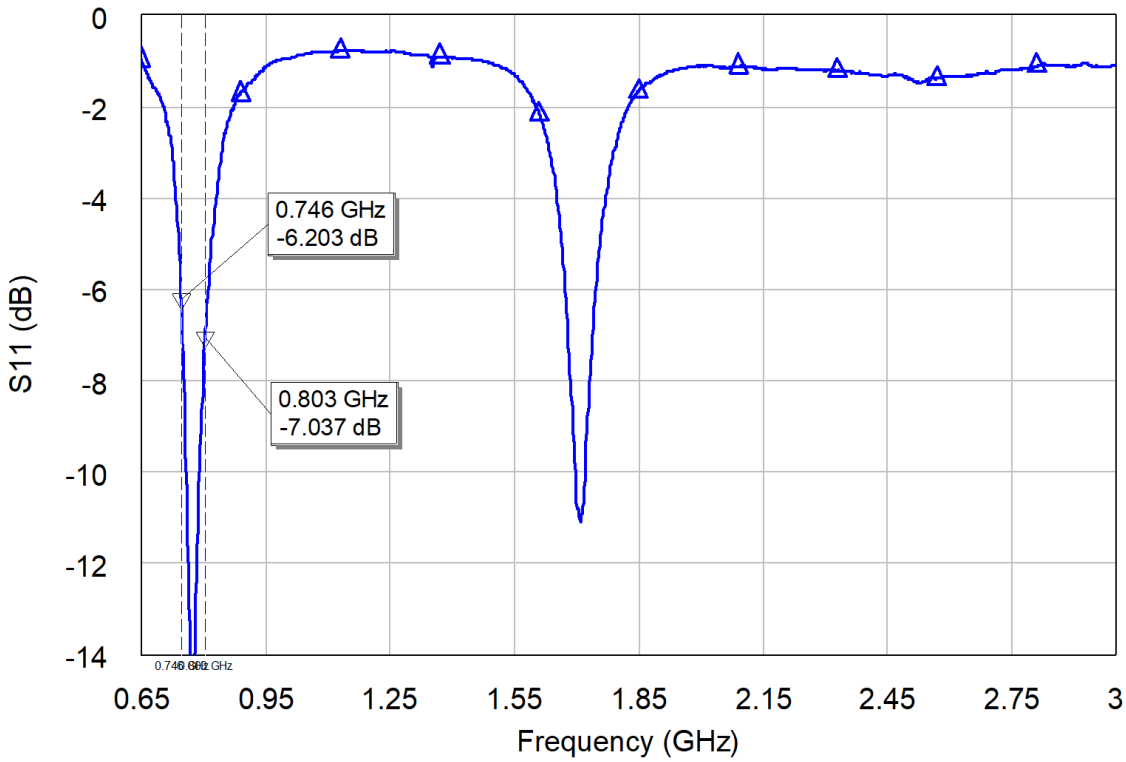

Figure 50 – Reflection coefficient for the Matching Network in Table 35.

4.3.2.3. Efficiency (%)

The antenna efficiency obtained at 746 – 803 MHz is 45.1%.

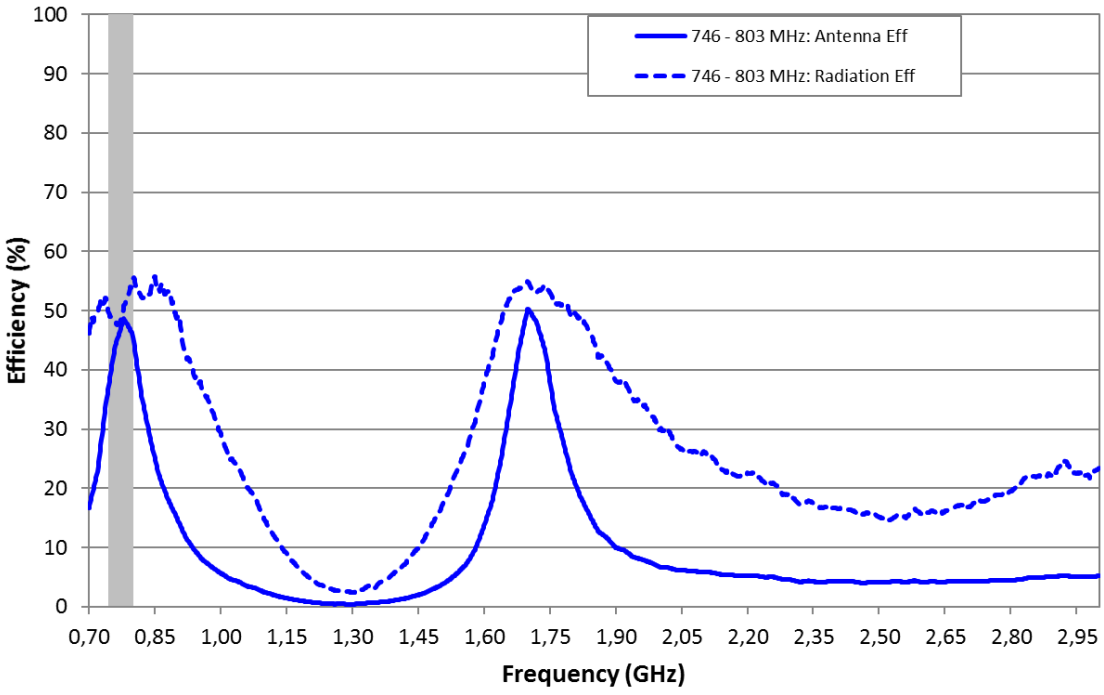

Figure 51 – Antenna and Radiation Efficiency (%) for the Matching Network (Table 35).

	Antenna Efficiency (%)				
Frequency range of interest	$\eta_{a\ 746\ MHz}$	$\eta_{a\ 803\ MHz}$	Min	Max	Av. η_a
746 – 803 MHz MN	37.4	44.8	37.4	48.7	**45.1**

Table 36 – Antenna efficiency (%) for the measured Matching Network for 746 – 803 MHz on the prototype shown in Figure 47.

4.3.3. 791 – 849 MHz

4.3.3.1. Matching network

For the case of 791 – 849 MHz, the two-component matching consists of a series inductor and a shunt capacitor (Table 37).

Component	Value	P/N
Z1	19 nH	LQW18AN18NG80
Z2	4.5 pF	GJM1555C1H4R5WB01
Z3	0Ω	-
Z4	Empty	-
Z5	0Ω	-
Z6	Empty	-
Z7	Empty	-
Z8	0Ω	-

Table 37 – Measured Matching Network values for 791 – 849 MHz of the Fleet Management PCB size prototype.

4.3.3.2. Reflection coefficient

For 791 – 849 MHz, it is reached S_{11} (dB) < -6dB with deep matching in the center of the band. A resonance appears at 1.35GHz, which is due to the transmission line.

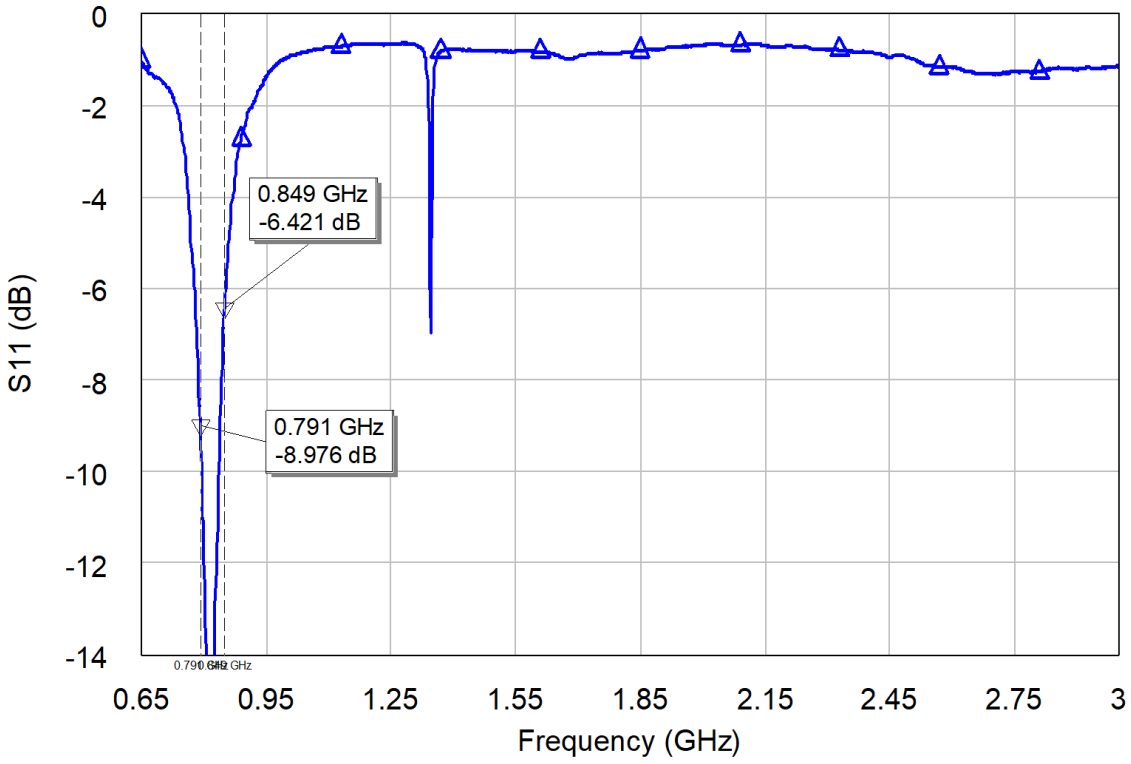

Figure 52 – Reflection coefficient for the Matching Network in Table 37.

4.3.3.3. Efficiency (%)

The antenna efficiency obtained for 791 – 849 MHz is 47.1%.

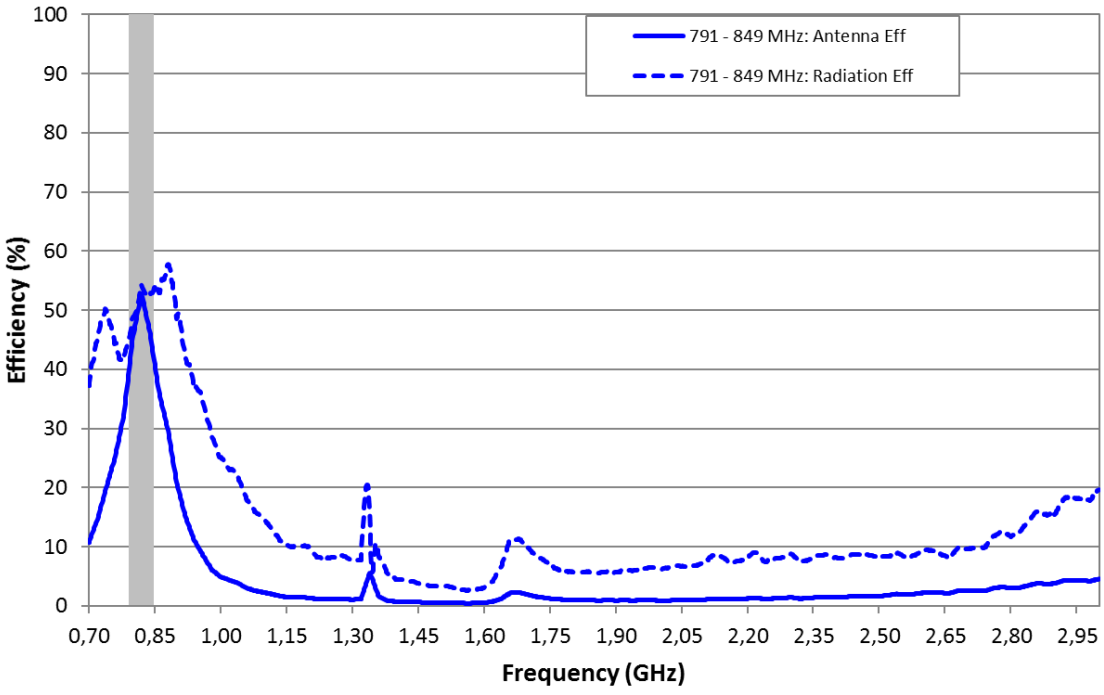

Figure 53 – Antenna and Radiation Efficiency (%) for the Matching Network (Table 37).

	Antenna Efficiency (%)				
Frequency range of interest	$\eta_{a\ 791\ MHz}$	$\eta_{a\ 849\ MHz}$	Min	Max	Av. η_a
791 – 849 MHz MN	39.2	41.5	39.2	52.8	**47.1**

Table 38 – Antenna efficiency (%) for the measured Matching Network for 791 – 849 MHz on the prototype shown in Figure 47.

4.3.4. 824 – 894 MHz

4.3.4.1. Matching network

The two-component matching network for 824 – 894 MHz is formed by a series inductor and a shunt capacitor (Table 39).

Component	Value	P/N
Z1	15 nH	LQW18AN15NG80
Z2	4.5 pF	GJM1555C1H4R5WB01
Z3	0Ω	-
Z4	Empty	-
Z5	0Ω	-
Z6	Empty	-
Z7	Empty	-
Z8	0Ω	-

Table 39 – Measured Matching Network values for 824 – 894 MHz of the Fleet Management PCB size prototype.

4.3.4.2. Reflection coefficient

The corresponding reflection coefficient for 824 – 894 MHz is almost S_{11} (dB) < -6dB along the band (excluding the upper edge of the band). The resonance at 1.35GHz due to the transmission line is present in this case too.

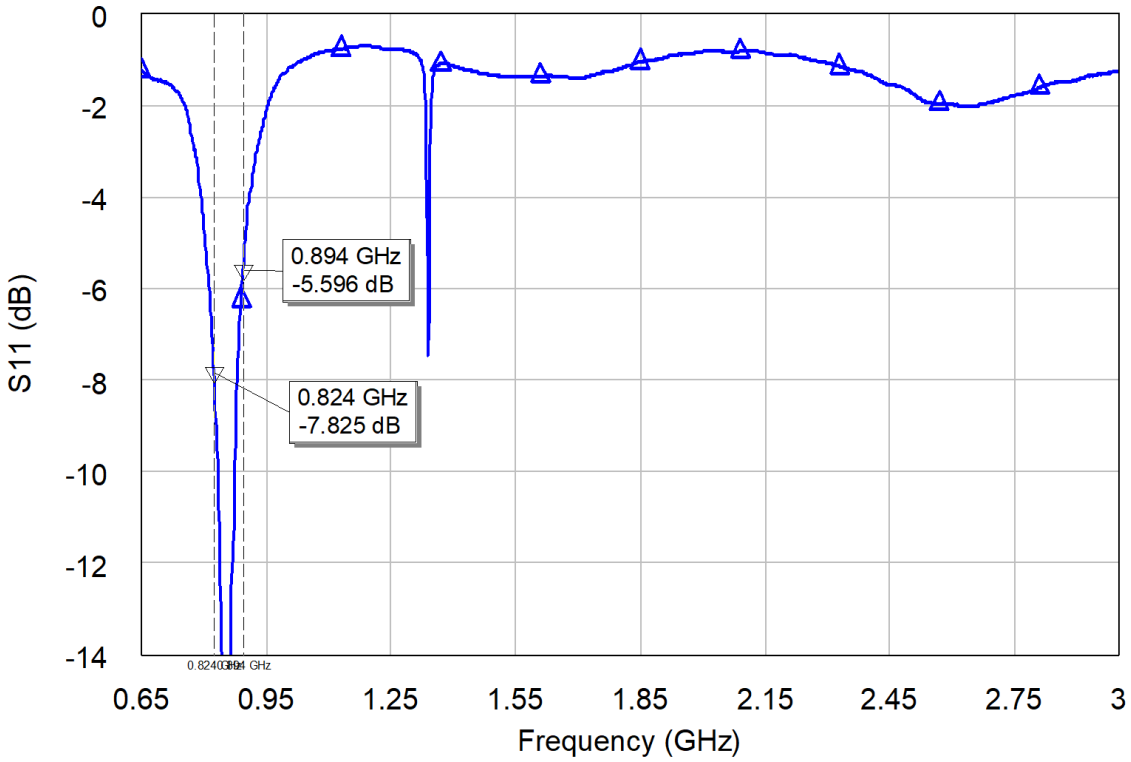

Figure 54 – Reflection coefficient for the Matching Network in Table 39.

4.3.4.3. Efficiency (%)

The achieved antenna efficiency for 824 – 894 MHz is 53.1%.

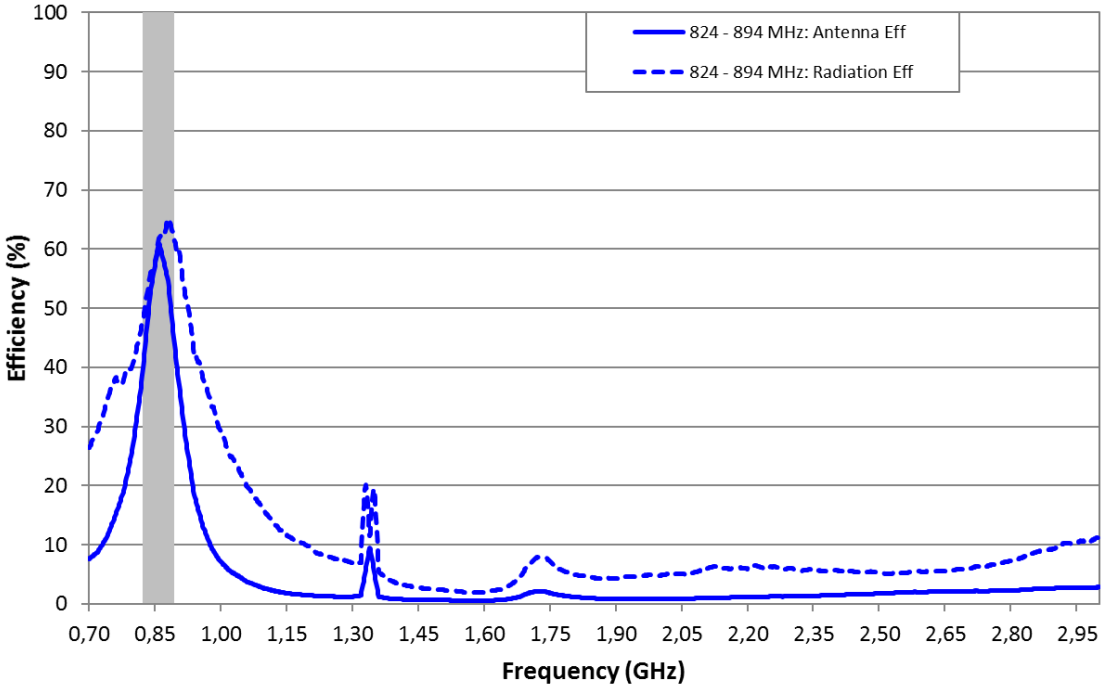

Figure 55 – Antenna and Radiation Efficiency (%) for the Matching Network (Table 39).

	Antenna Efficiency (%)				
Frequency range of interest	$\eta_{a\ 824\ MHz}$	$\eta_{a\ 894\ MHz}$	Min	Max	Av. η_a
824 – 894 MHz MN	39.9	44.9	39.9	60.9	**53.1**

Table 40 – Antenna efficiency (%) for the measured Matching Network for 824 – 894 MHz on the prototype shown in Figure 47.

4.3.5. 880 – 960 MHz

4.3.5.1. Matching network

The matching network for 880 – 960 MHz consists of a series inductor and a shunt capacitor (Table 41).

Component	Value	P/N
Z1	10 nH	LQW18AN10NG80
Z2	3.5 pF	GJM1555C1H3R5WB01
Z3	0Ω	-
Z4	Empty	-
Z5	0Ω	-
Z6	Empty	-
Z7	Empty	-
Z8	0Ω	-

Table 41 – Measured Matching Network values for 880 – 960 MHz of the Fleet Management PCB size prototype.

4.3.5.2. Reflection coefficient

Again, the reflection coefficient is below -6dB along the band of interest, with the resonance due to the transmission line at 1.35GHz.

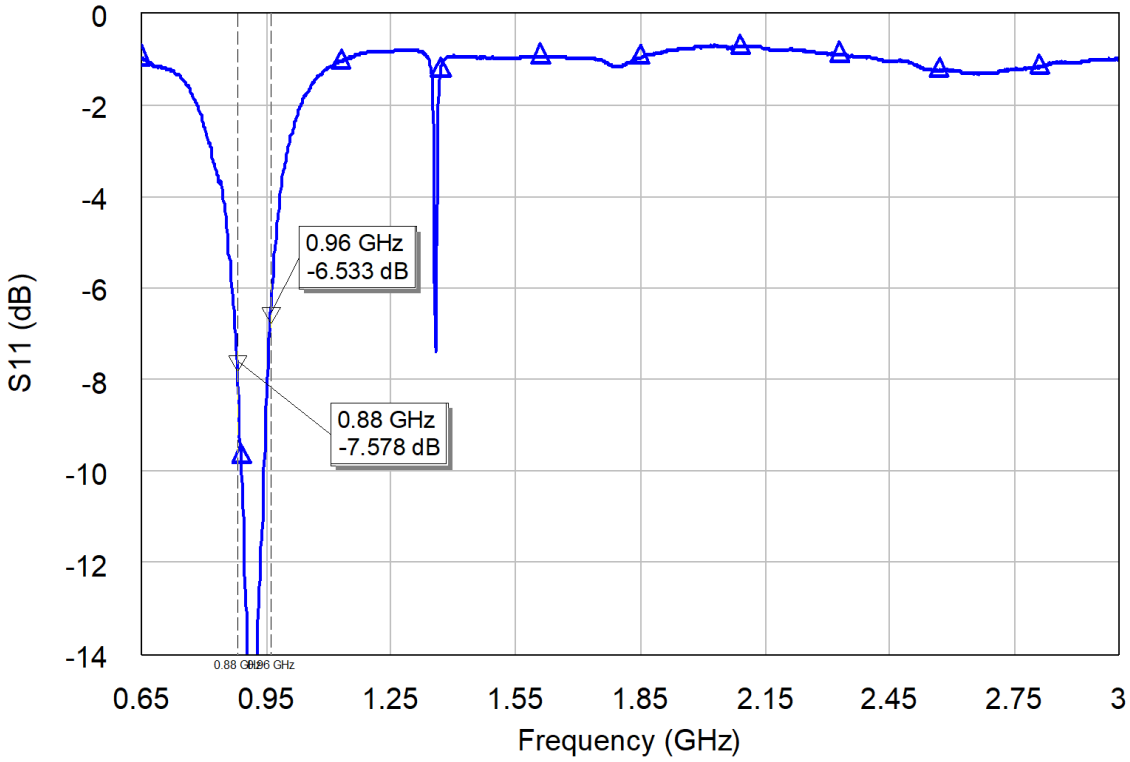

Figure 56 – Reflection coefficient for the Matching Network in Table 41.

4.3.5.3. Efficiency (%)

For the 880 – 960 MHz case, the achieved antenna efficiency gets to 61.9% (Figure 57).

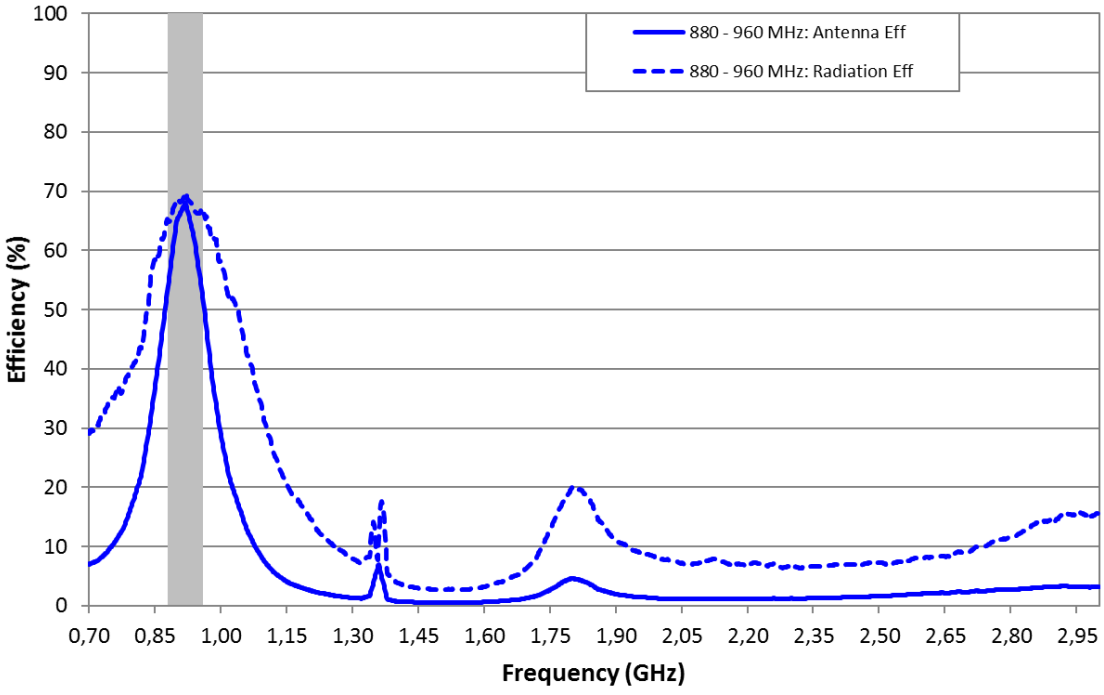

Figure 57 – Antenna and Radiation Efficiency (%) for the Matching Network (Table 41).

	Antenna Efficiency (%)				
Frequency range of interest	$\eta_{a\ 880\ MHz}$	$\eta_{a\ 960\ MHz}$	Min	Max	Av. η_a
880 – 960 MHz MN	54.0	52.1	52.1	68.1	**61.9**

Table 42 – Antenna efficiency (%) for the measured Matching Network for 880 – 960 MHz on the prototype shown in Figure 47.

4.3.6. 1710 – 2690 MHz

4.3.6.1. Matching network

The last of the selective matching networks, which covers 1710 – 2690 MHz, consist in a series inductor and a shunt capacitor too (Table 43).

Component	Value	P/N
Z1	6 nH	LQW18AN6NG80
Z2	0.4 pF	GJM1555C1HR40WB01
Z3	0Ω	-
Z4	Empty	-
Z5	0Ω	-
Z6	Empty	-
Z7	Empty	-
Z8	0Ω	-

Table 43 – Measured Matching Network values for 1710 – 2690 MHz of the Fleet Management PCB size prototype.

4.3.6.2. Reflection coefficient

The corresponding reflection coefficient to the matching network in Table 43 is below -7dB along all the region of interest. The resonance of the transmission line at 1.35GHz is present too.

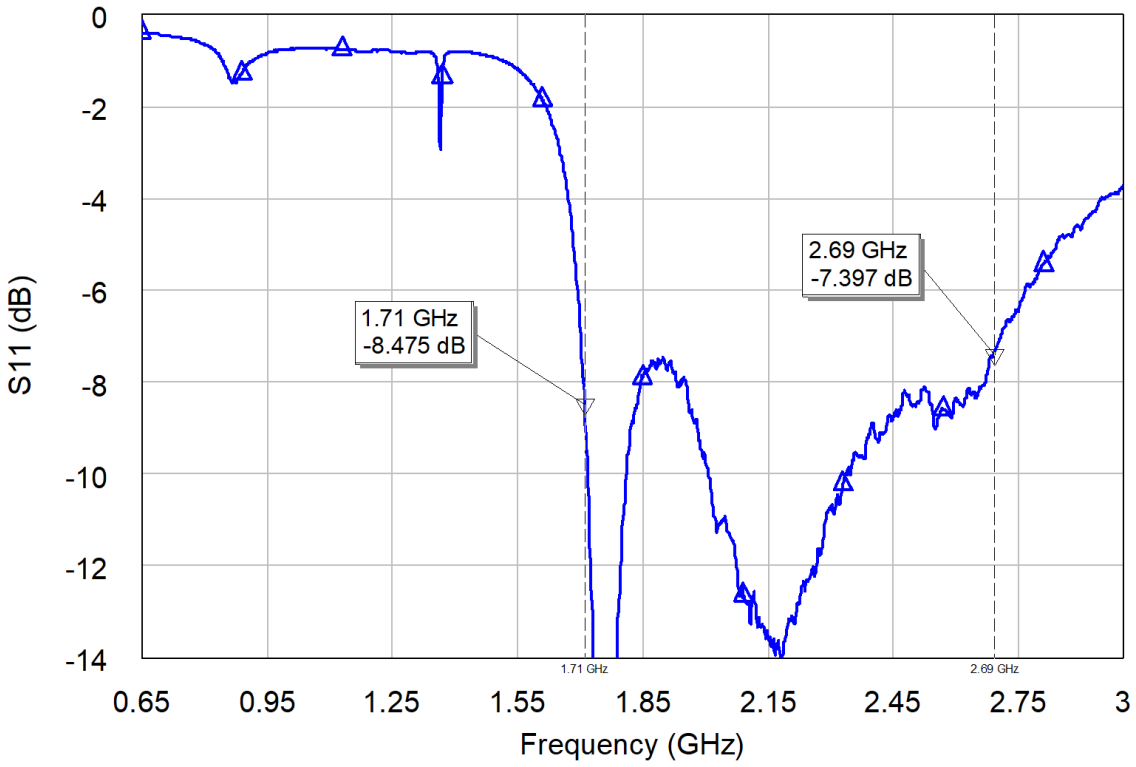

Figure 58 – Reflection coefficient for the Matching Network in Table 43.

4.3.6.3. Efficiency (%)

The average antenna efficiency reached in the HFR (1710 – 2690 MHz) with the two-component matching network presented in Table 43 is 69.9% (Figure 59).

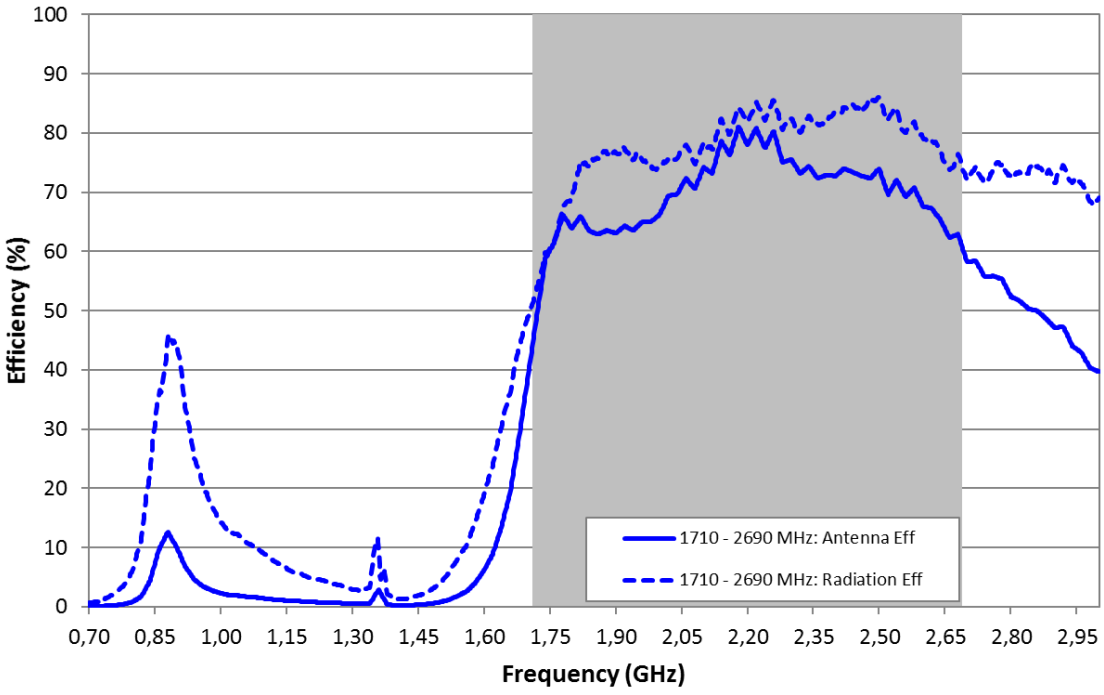

Figure 59 – Antenna and Radiation Efficiency (%) for the Matching Network (Table 43).

	Antenna Efficiency (%)				
Frequency range of interest	η_{a} 1710 MHz	η_{a} 2690 MHz	Min	Max	Av. η_{a}
1710 – 2690 MHz MN	43.9	60.7	43.9	81.0	**69.6**

Table 44 – Antenna efficiency (%) for the measured Matching Network for 1710 – 2690 MHz on the prototype shown in Figure 47.

4.3.7. Summary

After implementing the active solution for all the bands on the prototypes, the envelope of the efficiencies obtained for each band is traced to figure out the actual performance that this solution offers and to compare it with the classical passive solution.

In Figure 60 is shown the envelope of the antenna efficiency (%), where are traced the antenna efficiency that has been obtained for each band. For the overlapped frequencies (for instance: between the 698 – 748 MHz and the 746 – 803 MHz, there is overlapping in 746 – 748 MHz), it has been taken the maximum value. This is obtained by considering that the switches are lossless.

For the sake of having more realistic results that can be actually obtained using this configuration, it has been introduced 0.3dB of losses for each of both the switches that would be integrated.

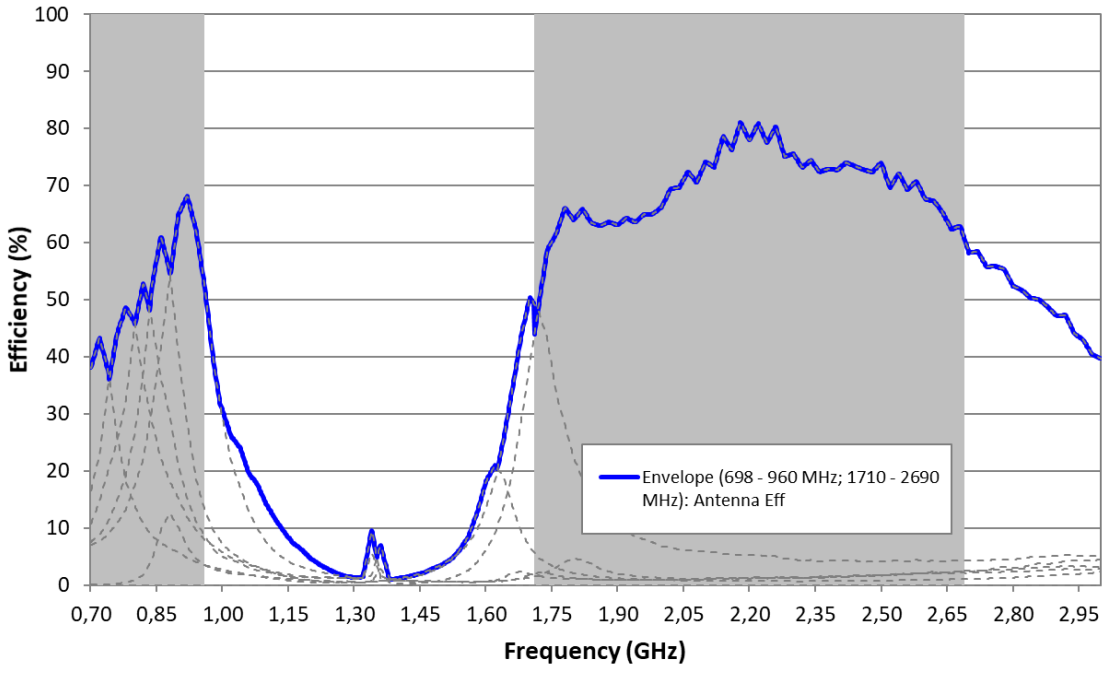

Figure 60 – Envelope of the Antenna Efficiency (%) of the active solution for Fleet Management PCB size prototype considering lossless switches.

	LFR (698 – 960 MHz)					HFR (1710 – 2690 MHz)				
Frequency range of interest	**$\eta_{a\ 698\ MHz}$**	**$\eta_{a\ 960\ MHz}$**	**Min**	**Max**	**Av. η_a**	**$\eta_{a\ 1710\ MHz}$**	**$\eta_{a\ 2690\ MHz}$**	**Min**	**Max**	**Av. η_a**
Lossless	38.1	52.1	38.1	68.1	**52.1**	43.9	60.7	43.9	81.0	**69.6**

Table 45 – Antenna efficiency (%) of the active solution for the Fleet Management PCB size prototype considering lossless switches.

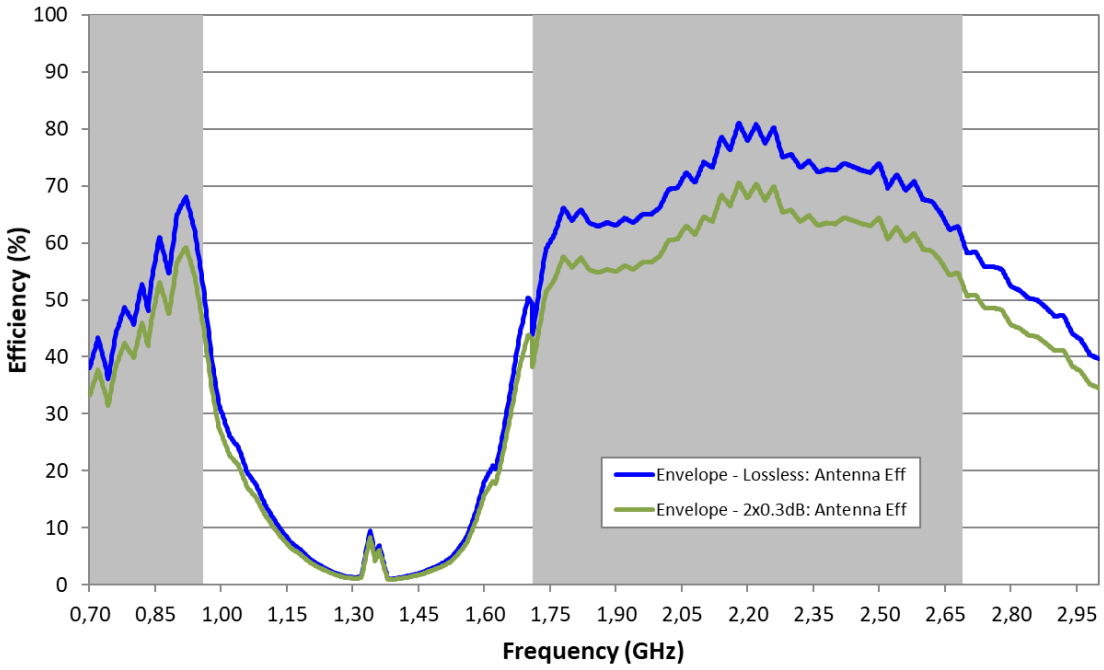

Figure 61 – Envelope of the Antenna Efficiency (%) of the active solution for Fleet Management PCB size prototype considering 0.3dB of insertion loss for each of the switches.

As seen in Figure 61 and Table 46, the effect of the losses that the switches introduce are reflected as a decrease of 6.7% at the LFR in the efficiency, while the HFR suffers a drop of 8.7% respect to the lossless switches' case. In this case, switches are taken from Qorvo [37].

	LFR (698 – 960 MHz)					HFR (1710 – 2690 MHz)				
Frequency range of interest	**$\eta_{a\ 698\ MHz}$**	**$\eta_{a\ 960\ MHz}$**	**Min**	**Max**	**Av. η_a**	**$\eta_{a\ 1710\ MHz}$**	**$\eta_{a\ 2690\ MHz}$**	**Min**	**Max**	**Av. η_a**
Lossless	38.1	52.1	38.1	68.1	**52.1**	43.9	60.7	43.9	81.0	**69.6**
IL = 2x(-0.3dB)	33.2	45.3	31.4	59.3	**45.4**	38.2	52.9	38.2	70.6	**60.9**

Table 46 – Antenna efficiency (%) of the active solution for the Fleet Management PCB size prototype considering lossless switches.

4.4. Conclusions

In this chapter the active solution has been implemented to improve the efficiencies that can be obtained by the classical passive solution with a broadband matching network.

From the simulations, it is appreciable that the active solution provides better performance in terms of efficiency than the passive solution (Figure 46). This improvement is vastly visible on the LFR (698 – 960 MHz) (Figure 35, Figure 37, Figure 39, Figure 41 and Figure 43), where the reflection coefficient is highly improved and, consequently, so does the efficiency. Moreover, the HFR (1710 – 2690 MHz) is also slightly improved (Figure 45).

On the other hand, from the measurements of the prototypes (Figure 62) it has been obtained the efficiency of the active solution for the Fleet Management platform.
From Figure 61 and Table 46 is extracted that, after adding the effect of the losses that the switches introduce, the LFR (698 – 960 MHz) presents an average antenna efficiency of 45.4%. Moreover, the HFR's (1710 – 2690 MHz) performance in terms of average efficiency is 60.9%.

Figure 62 – Resulting prototypes from the measurements.

The differences between the simulated and measured matching networks, reflection coefficients and efficiencies are due to different causes:

- In the simulation, the dielectric loss of the used FR4 is taken as a constant respect to the frequency. In the reality, the dielectric loss is frequency dependent with huge variations.
- Apart from the tolerances of the components, which are contemplated in both simulations and measurements, the VNA and the anechoic chamber where the measurements have been taken have tolerances that are not present on the simulations.
- For the case of the simulations, the point where it is calculated the reflection coefficient and the efficiency is in the exact point where the matching network area ends. On the other hand, in the case of the measurements, a cable is connected between the matching network area end and the point of measurement. This cable may introduce some effect that change the performance of the system.

5. CONCLUSIONS

The main goal of this project was increasing the efficiency that small platforms offer when dealing with 4G frequencies. To achieve this requirement, several previous sub-objectives had to be achieved:

From the carried-out market study, it has been extracted the following delimitations:

- The developed work has been focused in Fleet Management devices, which reference size **80mm x 50mm**.
- The 4G frequencies to cover are the ranges **698 – 960 MHz (LFR)** and **1710 – 2690 MHz (HFR)**.

It has been carried out an analysis regarding the impact of the ground plane length on the performance, in terms of efficiency, of the system. This study proved that the performance decreases when shortening the ground plane. For the dimensions 80mm x 60mm, it is obtained the performance shown in Table 47.

	LFR (698 – 960 MHz)					HFR (1710 – 2690 MHz)				
Ground Plane dimensions (mm x mm)	**$\eta_{a\ 698\ MHz}$**	**$\eta_{a\ 960\ MHz}$**	**Min**	**Max**	**Av. η_a**	**$\eta_{a\ 1710\ MHz}$**	**$\eta_{a\ 2690\ MHz}$**	**Min**	**Max**	**Av. η_a**
80mm x 60mm	24.2	25.5	24.2	37.9	**31.2**	63.0	38.0	38.0	72.7	**62.5**

Table 47 – Antenna efficiency (%) for the 80mm x 60mm case.

After that, it has been explored the active solution, which helped to improve the efficiencies in order to achieve the >30%. It has been done for both simulations and measurements.
The achieved improvement when implementing this technique is very significative for both scenarios (simulations and measurements), as shown in Figure 46 and Figure 63 respectively.

For the case of the measurements, the final results of the active solution are compared to the 80mm x 60mm PCB size in Figure 63 and Table 48.

	LFR (698 – 960 MHz)					HFR (1710 – 2690 MHz)				
Case	**$\eta_{a\ 698\ MHz}$**	**$\eta_{a\ 960\ MHz}$**	**Min**	**Max**	**Av. η_a**	**$\eta_{a\ 1710\ MHz}$**	**$\eta_{a\ 2690\ MHz}$**	**Min**	**Max**	**Av. η_a**
80mm x 60mm (passive solution)	24.2	25.5	24.2	37.9	**31.2**	63.0	38.0	38.0	72.7	**62.5**
80mm x 50mm (active solution)	33.2	45.3	31.4	59.3	**45.4**	38.2	52.9	38.2	70.6	**60.9**

Table 48 – Antenna efficiency (%) comparison between the passive and envelope of the active solution regarding 80mm x 60mm and 80mm x 50mm dimensions respectively.

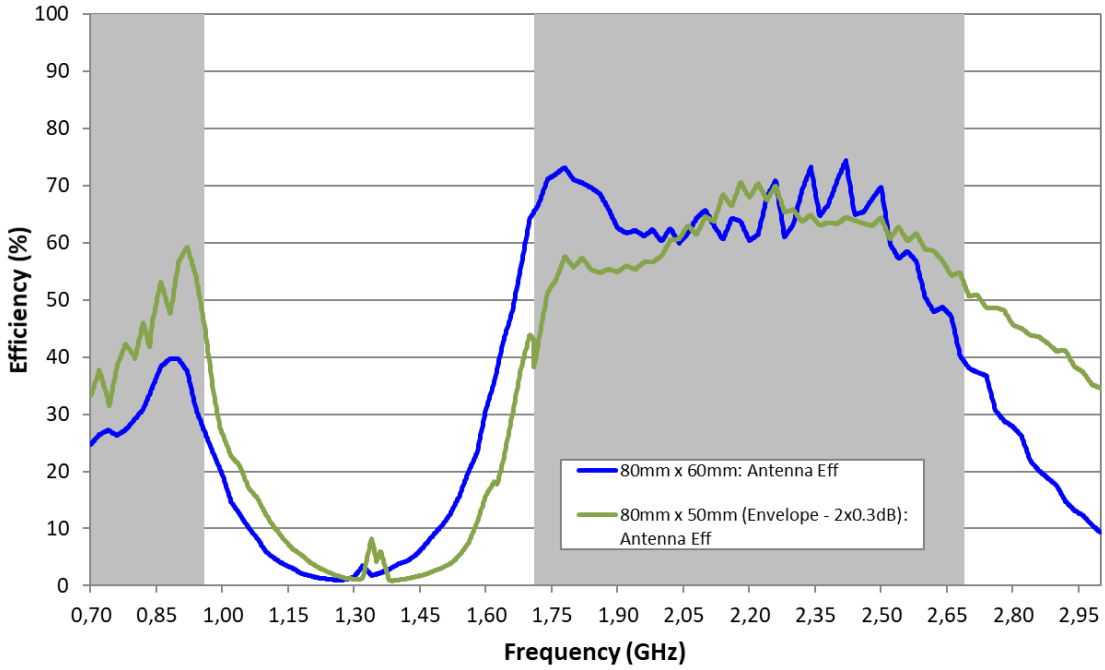

Figure 63 – Antenna Efficiency (%) comparison: 80mm x 60mm (passive solution) vs. 80mm x 50mm (envelope of active solution).

The active solution has helped to achieve the objective of the project without adding a very high complexity component to the system.
It is a technique that is currently being used for projects with real full designs and it is getting more and more attention from the designers.
For such small platforms, it can be the difference between being able to pass an EMC (Electromagnetic Compatibility) certification or not, which may be a very critical point in the development of a device.

5.1. Future lines

As further work that could be done in the future, it would be interesting to implement the active solution for the other applications that have been analyzed in the benchmarking phase (Modules, OBDs and IoT devices).

REFERENCES

[1]. CST – Computer Simulation Technology, Dassault Systemes, accessed 30th June 2019, https://www.cst.com/

[2]. RUN mXTEND™ product page, Fractus Antennas, accessed 30th June 2019, https://www.fractusantennas.com/mobile-antenna/

[3]. TRIO mXTEND™ product page, Fractus Antennas, accessed 30th June 2019, https://www.fractusantennas.com/trio-mxtend-mobile-iot-antenna/

[4]. J. Anguera, N. Toporcer, and A. Andújar, "Slim booster bars for electronic devices", US Patent 9,960,478.

[5]. J. Anguera, A. Andújar, C. Puente, and R. Mateos, "Modular multi-stage antenna system and component for wireless communications", patent App. US62/529,032.

[6]. ALL mXTEND™ product page, Fractus Antennas, accessed 30th June 2019, https://www.fractusantennas.com/lte-antenna/

[7]. J. Anguera, A. Andújar, M.C. Huynh, C. Orlenius, C. Picher, and C. Puente, "Advances in Antenna Technology for Wireless Handheld Devices", International Journal Antennas Propag., Vol. 2013, Article ID 838364.

[8]. J. Anguera, I. Sanz, J. Mumbrú, and C. Puente, "Multi-Band Handset Antenna with a Parallel Excitation of PIFA and Slot Radiators", IEEE Trans. Antennas and Propag., vol.58, no. 2, pp.348-356, Feb.2010.

[9]. A. Andújar, J. Anguera and C. Puente, "Ground-Plane Boosters as a Compact Antenna Technology for Wireless Handheld Devices," IEEE Trans. Antennas and Propag., Vol. 59, no. 5, May 2011, pp. 1668-1677.

[10]. C. Picher, J. Anguera, A. Bujalance, A. Andújar, "Ground Plane Booster Antenna Technology using a Self-Diplexed Matching Network for Multiband Operation", Microw. Opt. Tech. Letters, vol.58, no. 2, pp.453-461, February 2016.

[11]. J. Anguera, C. Picher, A. Bujalance, and A. Andújar, "Ground Plane Booster Antenna Technology for Smartphones and Tablets", Microw. Opt. Tech. Letters, vol.58, no. 6, pp.1289-1294, June 2016.

[12]. J. Anguera and A. Andújar, "Ground Plane Contribution in Wireless Handheld Devices using Radar Cross Section Analysis", Progress In Electromagnetics Research M, vol.26, pp-101-114, 2012.

[13]. A. Andújar and J. Anguera, "Magnetic Boosters for Multi-band Operation", Microw. Opt. Tech. Letters, vol.55, no. 1, pp.65-75, January 2013.

[14]. A. Andújar and J. Anguera, "Multiband Coplanar Ground Plane Booster Antenna Technology", Electron. Letters, vol.48, no. 21, pp. 1326-1328, Oct. 2012.

[15]. J. Anguera, A. Andújar, and C. García, "Multiband and Small Coplanar Antenna System for Wireless Handheld Devices", IEEE Trans. Antennas Propag., vol.61, no. 7, pp. 3782-3789, July 2013.

[16]. C. Picher, J. Anguera, A. Andújar, C. Puente, and A. Bujalance, "Concentrated Ground Plane Booster Antenna Technology for Multiband Operation in Handset Devices", Radioengineering, Vol. 23, no. 4, Dec. 2014. pp.1061-1070.

[17]. A. Andújar and J. Anguera, "Integration of a Non-Resonant Antenna in a Smartphone for Multiband Operation", European Conference Antennas and Propagation, EUCAP, London, UK, April 2018.

[18]. J. Anguera, A. Andújar, J.L. Leiva, C. Schepens, R. Gaddi, S. Kahng, "Multiband Antenna Operation with a Non-Resonant Element Using a Reconfigurable Matching Network", European Conference on Antennas and Propag., EUCAP, London, UK, April 2018.

[19]. J. Anguera, A. Andújar, J. Rahola, J. Juntunen, “Synthesis of Multiband Matching Networks for Non-Resonant Antennas”, Computing and Electromagnetics CEM’17, Barcelona, Spain, June 2017.

[20]. A. Andújar, J. Anguera, and R. Mª Mateo, “Multiband Non-Resonant Antenna System with Reduced Ground Clearance”, European Conference on Antennas Propag., EUCAP, Paris, France, April 2017.

[21]. J. Anguera, A. Andújar, R. Mª Mateo, and S. Kahng, “A 4 x 4 MIMO Multiband Antenna System with Non-Resonant Elements for Smartphone Platforms”, European Conference on Antennas Propag., EUCAP 2017, Paris, France, April 2017.

[22]. L. Grau, A. Andújar, and J. Anguera, “On the Isolation of a MIMO 2 x 2 Antenna System using Non-Resonant Elements: 1.71GHz-2.69GHz case study”, Microw. Opt. Tech. Letters, vol. 59, no. 9, pp.2348-2353, Sep. 2017.

[23]. J. Anguera, A. Andújar, and C. Puente, “Antenna-Less Wireless: A Marriage Between Antenna and Microwave Engineering”, Microwave Journal (invited paper), vol.60, no.10, October 2017, pp.22-36.

[24]. A. Andújar, Y. Cobo, and J. Anguera, “Effects of a Phantom Hand on a Non-Resonant Element for a 2.5GHz Smartwatch Antenna”, Intl. Journal of Electron. Comm., vol. 98, pp. 1-7, Jan 2019.

[25]. J. Anguera, A. Andújar, G. Mestre, J. Rahola, J. Juntunen, “Design of Multiband Antenna Systems for Wireless Devices Using Antenna Boosters”, IEEE Microw. Magazine, accepted paper, 2019.

[26]. J. Anguera, A. Andújar, C. Puente, and J. Mumbrú, “AntennaLess Wireless Device”, US. Patent US8203492 (B2), 2008, US9130259 (B2); US9276307 (B2); US9761944 (B2); US15/973124 (A1).

[27]. J. Anguera, A. Andújar, C. Puente, and J. Mumbrú, “AntennaLess Wireless Device Capable of Operation in Multiple Frequency Regions”, US Patent 8,237,615, 2008 (B2); CN102084542 (B2); EP09777590.2 (A1); US8736497 (B2); US9350070 (B2); US9960490 (B2); US15927497 (A1)

[28]. J. Anguera, C. Borja, C. Picher, and A. Andújar, “Wireless Device Providing Operability for Broadcasting Standards and Method Enabling such Operability”, China Patent CN104508905 (B2).

[29]. J. Anguera and A. Andújar, “AntennaLess Wireless Device Comprising One or More Bodies”, US9147929 (B2).

[30]. A. Andújar, J. Anguera, C. Puente, and C. Picher, “Wireless Device Capable of Multiband MIMO Operation”, CN103155276 (B2); US8952855 (B2); US9112284 (B2); US9997841 (B2).

[31]. A. Andújar and J. Anguera, “Compact Radiating Array for Wireless Handheld or Portable Devices”, US9577325 (B2); US15/415586 (A1).

[32]. J. Anguera, C. Picher, A. Andújar, and C. Puente, “Concentrated Antennaless Wireless Device Providing Operability in Multiple Frequency Regions”, CN104798251 (B2); EP13753587.8 (A1); US9379443 (B2); US15/608461 (A1).

[33]. A. Andújar and J. Anguera, “Scattered Virtual Antenna Technology for Wireless Devices”, US10062973 (B2).

[34]. J. Anguera, A. Andújar, and C. Puente, “Wireless handheld devices, radiation systems and manufacturing methods”, CN104508905 (B2); EP13762997.8 (A1); US9331389 (B2); US9865917 (B2); US15/835007 (A1).

[35]. Design Support Software SimSurfing, Murata, accessed 1st July 2019, https://ds.murata.co.jp/simsurfing/index.html?lcid=en-us

[36]. Tutorials – Design your antenna in 3 steps, Fractus Antennas, accessed 30th June 2019, https://www.fractusantennas.com/tutorials/

[37]. Qorvo, accessed 30th June 2019, https://www.qorvo.com